NATIONAL AERONAUTICAL ESTABLISHMENT
LIBRARY

C.P. No. 64
13064
A.R.C. Technical Report

[illegible]
– 5 [illegible] 1952
NR. [illegible]

MINISTRY OF SUPPLY

AERONAUTICAL RESEARCH COUNCIL
CURRENT PAPERS

The Measurement of Heat Transfer and Skin Friction at Supersonic Speeds

Part II. Boundary Layer Measurements on a Flat Plate at M = 2.5 and Zero Heat Transfer

By

R. J. Monaghan, M.A. and
J. E. Johnson, M.Sc.(Tech.), A.M.I.Mech.E.

Crown Copyright Reserved

LONDON: HIS MAJESTY'S STATIONERY OFFICE

1952

Eight Shillings Net.

NATIONAL AERONAUTICAL ESTABLISHMENT
LIBRARY

C.P. No. 64

Technical Note No. Aero.2031
Sup.99

December, 1949

ROYAL AIRCRAFT ESTABLISHMENT

The measurement of heat transfer and skin friction at supersonic speeds

Part II - Boundary layer measurements on a flat plate at M = 2.5 and zero heat transfer

by

R.J. Monaghan, M.A.
and
J.E. Johnson, M.Sc.(Tech.), A.M.I.Mech.E.

SUMMARY

The preliminary heat transfer investigation, reported in the first note[1] of this series, was made with a heated copper plate let into one wall of a supersonic tunnel and in the tunnel boundary layer.

This note describes the subsequent design modifications made to remove this layer at the leading edge of the plate and gives the results of pitot traverses in the ensuing fresh boundary layer. The tests were made on an unheated wooden plate under zero heat transfer conditions at M = 2.5.

The measured rate of growth of the laminar layer was greater than theory would predict. Transition to turbulent flow occurred between three and four inches from the leading edge, at a Reynolds number between 8×10^5 and 10^6.

The thickness of the turbulent layer was approximately the same as in low speed flow. Skin friction, deduced from the pitot traverses, was about 20 per cent below that obtained in Ref.1, and the mean coefficient agrees with a semi-empirical formula

$$C_{F_W} = 0.46\ (\log_{10} Re_W\ {}^{T_1}/T_W)^{-2.6}$$

where subscript "w" denotes wall temperature conditions

T_W is wall temperature

and T_1 is free stream temperature.

A preliminary investigation was made of the use of chemical methods for indicating transition.

LIST OF CONTENTS

Page

1 Introduction 4

2 Experimental apparatus 4

2.1 Unheated plate and suction slot 4
2.2 Pitot tubes 4
2.3 Measurement of stagnation pressure and temperature 5

3 Removal of the tunnel boundary layer at the leading edge of the plate 5

3.1 Weight flow of the air in boundary layer 5
3.2 Modification of slot and leading edge 5

4 Airflow over plate 6

5 Boundary layer measurements 7

5.1 Reduction of pitot measurements 7
5.2 Accuracy of results 9

6 Discussion of results 9

6.1 Laminar region 10
6.2 Turbulent region 11

7 Conclusions 17

List of Symbols 20
References 21

LIST OF APPENDICES

App.

Chemical indication of transition I

Derivation of formulae for turbulent skin friction etc. II

LIST OF TABLES

Table

Measurements of boundary layer on dummy hot plate I

Preliminary results from re-designed tunnel II

LIST OF ILLUSTRATIONS

	Fig.
Modification of slot for removal of tunnel boundary layer	1
Velocity profile and weight flow of air in boundary layer $\frac{1}{4}$" ahead of slot	2
Pressure distribution through suction slot and pipe	3
Mach number variation along plate	4
Velocity profiles in boundary layer over forward portion of plate	5
Velocity profiles over rear portion of plate	6
Variation of displacement thickness	7
Variation of momentum thickness	8
Velocity profiles (log-law)	9
Mean skin friction coefficient	10
Ratio of displacement thickness to momentum thickness	11
Effect of pitot tube size on accuracy of boundary layer measurements	12
Chemical indication of transition using azobenzene	13

1 Introduction

The preliminary investigation of the heat transfer from a flat plate to an air stream at $M = 2.5$, reported in the first note[1] of this series, was made with a heated copper plate let into one wall of a supersonic tunnel. It had been hoped to remove the tunnel wall boundary layer by suction at the leading edge of the plate but, with the original design of suction slot (Fig.1a) and with the pump capacity available, it was found impossible to remove any appreciable proportion of it. Thus the tests were made with a turbulent boundary layer (approximately 0.2 in. thick) already in existence at the leading edge.

After the conclusion of the heat transfer tests, a detailed investigation of this boundary layer was made, using a similar unheated wooden plate. This showed that a considerable variation in boundary layer thickness and rate of growth could be caused by disturbances arising at the slot and from leakage of the joints between plate and tunnel. These quantities were unknown during the heat transfer tests so that generalisation of the results was impossible.

In order to determine the correct design of slot and suction pipe to remove the boundary layer and to obtain more information about the zero heat transfer condition, a fairly lengthy series of tests has been made using the unheated plate before proceeding with further tests on the hot plate. The results are given in this note and include estimates of turbulent skin friction (derived indirectly from pitot traverses) which are in good agreement with a semi-theoretical estimate. The results of a preliminary investigation of the use of chemical methods for indicating transition are given in Appendix I.

2 Experimental apparatus

Details of the tunnel, manometers and pressure connections etc., are given in Ref.1. The working section is 5 x 5 inches and 18 inches long. The nozzle is designed for $M = 2.5$ and in each test the stagnation temperature was adjusted to give zero heat transfer at the plate in accordance with the results of Ref.1.

2.1 Unheated plate and suction slot

The unheated plate is made of hard polished wood and was originally of the same external dimensions as the heated copper plate of Ref.1. In the original design the plate was mounted with its surface level with the tunnel wall and the shape of the leading edge and suction slot is shown in Fig.1a. There had to be a trailing entry to the slot because of the presence of the plate.

After the tests described in section 3, the plate was raised 0.16 inches and the final design of suction slot and modification of the leading edge is shown in Fig.1b. Four static pressure holes were fitted at the fore-and-aft positions indicated in Fig.4 (relative to the new leading edge). Their lateral position was along the line of the pitot traverses.

2.2 Pitot tubes

The pitot heads were made from hypodermic tubing of 0.02 inches outside diameter and were traversed through the boundary layer by means of a micrometer screw which read to 1/1000 inch. Full details of the traversing gear are given in Figs. 5 and 6 of Ref. 2. Some later check tests on the effect of pitot tube size were made with the same tubing flattened and filed to a height of 0.01 inches.

Three positions for fitting the traversing gear (in the opposite wall to the plate) were provided at 2, 6 and 11 inches behind the leading edge and pitot tubes of various lengths were made so that readings could be obtained at other positions.

2.3 Measurement of stagnation pressure and temperature

The stagnation pressure and temperature were measured in the same way as described in section 3.1 of Ref. 1.

3 Removal of the tunnel boundary layer at the leading edge of the plate

The original design of the leading edge of the plate and boundary layer sunction slot is shown in Fig. 1a and, when the tunnel was running, a weak oblique shock wave was present just ahead of the lip of the slot.

3.1 Weight flow of air in boundary layer

To make an estimate of the weight flow of air in the boundary layer approaching the slot, several pitot traverses were made just ahead of the shock wave. The resulting mean velocity profile (determined from the pitot measurements as in section 5 below, using the static pressure from point "A" of Fig.1a) is shown by the upper curve of Fig. 2. It is turbulent in form and the thickness of the layer is of the order of 0.25 inches. The average value of displacement thickness (δ^x) is 0.0435 inches.

Estimates of weight flow (lb/sec) across a section the width of the tunnel and of height y inches (from the wall) were calculated using the mean velocity profile and assuming constant total energy. The results are given by the lower curve* of Fig. 2.

To remove the whole of the boundary layer (up to $y = 0.25$ inches) would therefore involve removing 0.126 lb/sec of air.

3.2 Modification of slot and leading edge

The static pressure in the tunnel is of the order of 50 mm Hg. absolute and the pitot traverses of section 3.1 showed that the airflow in the boundary layer approaching the slot is supersonic to within 0.01 inches of the wall. When the original design of slot (Fig. 1a) was found to be impracticable it was decided to try the effect of raising the plate above wall level and fitting a sharp edged forward facing lip on to its leading edge (as in Fig. 1b). Compression to subsonic flow could then occur across a shock wave at the new entry and if the duct and piping losses were reduced, it was possible that the rise in pressure would enable a good proportion of the boundary layer to be removed by use of a reasonable pump capacity.

---

* The asymptote to this curve for large values of y is obtained by assuming that

$$u = 0 \text{ for } y < \delta^x$$

$$u = u_1 \text{ for } y > \delta^x$$

where u_1 is the free stream velocity.

The pressure losses in the suction system were reduced by enlarging the height of the slot and the diameter of the suction pipe. A steel tip 0.03 inches thick, ground to a knife edge, was fitted flush with the surface of the plate which was raised above the wall level. These modifications proved successful and a series of tests was made to determine the best fore-and-aft position for the knife edge, while the plate height was adjusted (using Fig.2) to suit the measured flow quantity through the pumps. The final modification of the system is shown in Fig.1b. In it the plate is raised 0.16 inches and the knife edge is vertically over the lip of the slot. A shadowgraph showed that in action there is a slightly concave shock between the two.

Ideally the plate should be raised 0.25 inches, but the maximum weight flow that could be obtained was of the order of 0.08 lb/sec and Fig.2 shows that this is sufficient for a plate height of 0.175 inches at most. The curves in Fig.2 give average values, so to allow for possible variations in pump performance the plate height was set at 0.16 inches.

Thus, not all of the boundary layer is removed but Fig.2 shows that the residue has at least 98-99% of the free stream velocity.

Fig.3 shows the pressure distribution obtained in the suction system after final modification. There is a large pressure rise under the tip but this is practically all lost in rounding the corner and passing through the slot. The losses in the rest of the system are small so that the pump pressure is about the same as the tunnel static pressure. The weight flow is measured by a 2 inch standard orifice in the 3 inch pipe. It was found that removing this orifice did not lead to an increase in pump pressure, so it was retained as a check on the efficiency of the system.

4 Airflow over plate

Fig.4 shows the variation of Mach number[*] along the wooden plate after removal of the tunnel boundary layer at the leading edge. The relevant points are classified under the heading "original nozzle", and are denoted by crosses.

A shadowgraph showed that there was a weak oblique shock wave at the leading edge of the plate. The shock angle was about 26° whereas for a Mach number of 2.48 (on tunnel wall ahead of shock) the Mach angle is 23.8°. Theoretically the Mach number behind the shock would then be 2.38. Fig.4 shows that the flow then expands to about $M = 2.5$ at five inches from the leading edge and afterwards falls away again. There was an insufficient number of static pressure holes on the plate to determine the variation with any accuracy, so the test results in the following sections are taken to apply at the mean Mach number.

$$M = 2.46$$

and the slight pressure gradients are neglected.

The mean value of Reynolds number, based on free stream conditions and a length of one inch is

$$2.5 \times 10^5$$

---

[*] derived from static pressure measurements at the surface of the plate.

Since the completion of the tests on the dummy plate, the tunnel has been re-designed with the aim of reducing the Mach number variation. The result is shown in Fig.4 under the heading "new nozzle". Aft of a point about 5 inches from the leading edge, the mean Mach number is

$$M_1 = 2.43$$

and the variation from it is very small.

Some of the preliminary results from the new tunnel are included in this report in order to strengthen the evidence on the turbulent boundary layer. They appear in Figs.7, 8, 10 and 11 and are denoted by circles to distinguish them from the main series of results which are denoted by crosses. In the analysis in this report, for simplicity the mean Mach number has been taken to be $M_1 = 2.46$ in all cases. Any errors thus introduced are likely to lie within the limits of experimental accuracy.

5 Boundary layer measurements. Zero heat transfer condition

Pitot traverses were made through the boundary layer at distances (x) downstream from the leading edge given in the first column of Tables I and II. The results of a preliminary investigation of the use of chemical methods for indicating the point of transition from laminar to turbulent flow are given in Appendix I. They indicate (Fig.13) that transition occurs at about $3\frac{1}{2}$ inches from the leading edge, which tallies with the pitot traverse results (section 6, below).

5.1 Reduction of pitot measurements

The original pitot measurements (Table I) were analysed to give velocity profiles (Figs.5, 6 and 9) and values of displacement thickness, momentum thickness and total skin friction (Table I and Figs.7, 8 and 10). Values of the latter quantities obtained in the re-designed tunnel are included in Figs.7, 8 and 10, and are tabulated in Table II.

Values of the velocity ratio u/u_1 (where subscript "1" denotes free stream conditions) were obtained from the pitot pressures and plate static pressures by using Rayleigh's pitot tube formula and by assuming constant total energy and static pressure across the boundary layer. For pitot positions that did not correspond to a measured static pressure, the value of the latter was obtained from a faired curve through the measured values.

Displacement thickness (δ^x) was calculated from the formula

$$\delta^x = \int_0^\delta \left(1 - \frac{\rho}{\rho_1}\frac{u}{u_1}\right) dy \qquad \ldots\ldots (1)$$

where
u is the velocity at a point in the boundary layer.

ρ is the density at the same point

y is the distance from the wall to this point (taken to be at the centre of the pitot orifice)

δ is the full boundary layer thickness

and subscript "1" refers to free stream conditions.

Momentum thickness (θ) was calculated from the formula

$$\theta = \int_0^{\delta} \frac{\rho u}{\rho_1 u_1} \left(1 - \frac{u}{u_1}\right) dy \qquad \ldots\ldots\ldots \quad (2)$$

In both these calculations it was necessary to assume constant total energy across the boundary layer in order to evaluate the density ρ.

If there is no pressure gradient along the plate then the local skin friction coefficient is given by

$$c_f = \frac{\tau_o}{\frac{1}{2}\rho_1 u_1^2} = 2\frac{d\theta}{dx} \qquad \ldots\ldots\ldots \quad (3)$$

where τ_o is the shearing stress at the surface of the plate.

By integration of equation (3) from the leading edge to position "x", we obtain the total skin friction coefficient

$$C_F = \frac{F}{\frac{1}{2}\rho_1 u_1^2 x} = 2\frac{\theta}{x} \qquad \ldots\ldots\ldots \quad (4)$$

which is considered in preference to the local coefficient because θ can be determined more accurately than $\frac{d\theta}{dx}$.

However, in obtaining the log-law velocity profiles of Fig.9, it was necessary to make estimates of $\frac{d\theta}{dx}$ and these were taken from the faired curves of Fig.8. These profiles (Fig.9) are of

$$u/u_{\tau_1} \text{ against } \log_{10} y_{\tau_1}$$

where

$$u_{\tau_1} = \left(\frac{\tau_o}{\rho_1}\right)^{\frac{1}{2}} \qquad \ldots\ldots\ldots \quad (5)$$

and

$$y_{\tau_1} = \frac{y u_{\tau_1}}{\nu_1} \qquad \ldots\ldots\ldots \quad (6)$$

where ν_1 is the kinematic viscosity evaluated at free stream temperature.

Finally, Reynolds number (Re_x) based on the length "x" is given by

$$Re_x = \frac{u_1 x}{\nu_1} \qquad \ldots\ldots \ (7)$$

and the free stream temperature is obtained from the stagnation temperature (T_c) by the formula

$$\frac{T_c}{T_1} = 1 + \frac{\gamma-1}{2} M_1^2 \qquad \ldots\ldots \ (8)$$

5.2 Accuracy of results

As mentioned in Ref.1, the assumption of constant total energy across the boundary layer in the zero heat transfer condition can introduce an error of up to 3% in the values of u/u_1 close to the surface. However, the errors in δ^x and θ arising from this source are of smaller order since each is obtained by an integration over the whole thickness of the layer.

The assumption of constant static pressure across the boundary layer seems to be valid except immediately behind the shock wave at the leading edge.

A more serious source of error might come from the application of Rayleigh's pitot tube formula to measurements from a pitot of finite size in a transverse velocity gradient as is the present case. Also, viscosity might influence the readings obtained with a small bore tube. To check these points, measurements were taken with pitots of two different sizes in both laminar and turbulent boundary layers. The resulting velocity profiles are shown in Fig.12 and there is no evidence of either a size or wall interference effect until the tube is touching the wall.* Any discrepancy between the profiles could be explained by an error in the zero position setting which is done visually and to the nearest 0.001 inch on the micrometer head.

The line of the pitot traverses was one inch off centre on the plate, but early tests showed that this position was free from interference from the thickened boundary layer at the junction of plate and side wall.

For these reasons it is considered that the results give a reasonably accurate estimate of conditions in the boundary layer.

6 Discussion of results

When the tunnel boundary layer has been removed at the leading edge of the plate and if the plate surface is smooth, it might be expected that the flow in the new boundary layer would be laminar for some distance back from the leading edge before becoming turbulent. Figs.5, 6, 7 and 8, show that there is in fact a change in velocity profile and in rate of growth of both displacement and momentum thickness at a distance between 3 and 4 inches from the leading edge.**

---

*This result is at slight variance with the measurements of Ref.2, which showed a size effect when the centre of the tube was within one tube diameter of the wall.

**As mentioned at the beginning of section 5, this checks with the chemical indication given in Fig.13 and discussed in Appendix I.

Based on the mean $M_1 = 2.46$, the free stream Reynolds number is approximately 2.5×10^5 per inch so that the transition value is between 8×10^5 and 10^6. The "laminar" and "turbulent" regions will be discussed separately in the following sub-sections.

6.1 Laminar region

In Fig.5 the velocity profiles over the forward portion of the plate are plotted as

$$u/u_1 \text{ against } y/x \sqrt{Re_x}$$

and are compared with the theoretical zero heat transfer laminar profile for $M_1 = 2.46$ obtained by the approximate method of Ref.3.

The profiles up to x = 3.0 inches roughly form a family, but do not agree with the theoretical profile and the boundary layer thickness is greater than would be predicted by theory. The same behaviour is exhibited by the results of Ref.2.

Figs.7 and 8 show a laminar variation of displacement and momentum thickness in this region but the absolute values are larger than the theoretical.[*] Thus the experimental values can be fitted by the curves

$$\delta^x = 5.5 \, Re_x^{-\frac{1}{2}} \, x$$

$$\text{and} \qquad \theta = Re_x^{-\frac{1}{2}} \, x$$

whereas theoretically[*]

$$\delta^x = 4.48 \, Re_x^{-\frac{1}{2}} \, x$$

$$\text{and} \qquad \theta = 0.63 \, Re_x^{-\frac{1}{2}} \, x \, .$$

Finally the experimental values of

$$H = \delta^x/\theta$$

shown in Fig.11, nowhere attain the theoretical laminar value of 7.1. (The large amount of scatter at x = 0.82 is caused by taking the two extremes of possible fairings to y = 0 of the curves used for determining δ^x and θ. As can be seen from Fig.5, only a limited number of experimental readings was available at this station because of the very thin boundary layer.)

These discrepancies may be caused by the presence of a shock of finite strength at the leading edge whereas the theory assumes that there is only a Mach line at that point. In fact, later experiments indicate that the thickness of the laminar layer may depend to a large extent on the condition of the knife edge and the exact setting of its height in relation to the flow quantity through the suction slot.

---

[*] obtained by the method of Ref.3.

At this stage therefore no explanation of the discrepancies will be sought and discussion will be confined to the turbulent layer which has not been found to be so sensitive to changes in the leading edge condition.

6.2 Turbulent Region

6.21 Analysis on basis of power law velocity profile

Aft of a point about four inches from the leading edge, the velocity profiles (Fig.6) are in good agreement with the 1/7th power law turbulent profile of incompressible flow. (The plots are of u/u_1 against y/δ^x, but on the basis of the 1/7th power law and by assuming constant total energy across the boundary layer, the ratio δ^x/δ has been evaluated as a function of Mach number in Ref.4. Hence

$$u/u_1 = (y/\delta)^{1/7}$$

$$= (\delta^x/\delta)^{1/7}(y/\delta^x)^{1/7}$$

and for $M_1 = 2.46$, Ref.4 gives

$$\delta^x/\delta = 0.28 \;).$$

This result agrees with the results of Refs.1 and 2. Plots of displacement and momentum thicknesses against distance from the leading edge of the plate are given in Figs.7 and 8. Fig.11 shows that in the turbulent region the ratio of displacement to momentum thickness is approximately 4.0 (under the test conditions).

As mentioned in section 4, results from later tests, made under improved airflow conditions, are included to strengthen the evidence. These are denoted by circles.

The experimental points of Figs.7 and 8 define mean curves with reasonable accuracy. Those shown were obtained by imposing the conditions that both should give the same effective start to the turbulent boundary layer and that the mean condition

$$\delta^x/\theta = 4.0$$

of Fig.11 should be satisfied. When this is done it is found that the best position for the effective start is one inch back from the leading edge and that both δ^x and θ vary approximately as $X^{0.8}$, where $X = x - 1$. The final curves are

$$\delta^x = 0.106 \, Re_X^{-1/5} \, X \qquad \ldots\ldots\ldots (9)$$

and

$$\theta = 0.0265 \, Re_X^{-1/5} \, X$$

where $X = x - 1$.

Thus the incompressible flow correspondence between

$$u/u_1 = (y/\delta)^{1/7}$$

and

$$\frac{\delta^x}{x} \text{ or } \frac{\theta}{x} \propto \mathrm{Re}_x^{-1/5}$$

can be retained in compressible flow.

From Ref.4, at $M_1 = 2.46$

$$\delta^x/\delta = 0.28$$

and $$\theta/\delta = 0.07,$$

hence from equations 9 and 10 we obtain

$$\delta = 0.378\ \mathrm{Re}_x^{-1/5} x \qquad \ldots\ldots\ldots\ldots(12)$$

which compares with the low speed flow value (Ref.5)

$$\delta = 0.37\ \mathrm{Re}_x^{-1/5} x \qquad \ldots\ldots\ldots\ldots(13)$$

This result indicates that there is very little change in turbulent boundary layer thickness in changing from low speed to a Mach number of 2.5, and suggests that a good approximation to the variation of δ^x and θ with M should be given by the curves of δ^x/δ and θ/δ against M in Ref.4. If so, then, with increasing M, δ^x increases and θ (and hence C_F) decreases. Simple analytical expressions for these variations are found from the more general treatment of the following sub-section.

6.22 Analysis on basis of log-law velocity profile

The various power law velocity profiles of incompressible flow are only approximations, each valid within a limited range of Reynold's number, to the more general log-law profile

$$u/u_\tau = A + B \log_{10} y_\tau \qquad \ldots\ldots\ldots\ldots(14)$$

where

$$u_\tau = (\tau_o/\rho)^{\frac{1}{2}}$$

and

$$y_\tau = yu_\tau/\nu$$

The best agreement with low speed experimental results (mainly for pipe flows) over a wide range of Reynolds number has been found5 with

$$A = 5.5$$

and $$B = 5.75\ .$$

A further analysis of the present experimental results was therefore made on the basis of equation (14). Density and viscosity were evaluated at free stream temperature and values of τ_o were obtained by differentiation of the faired curve of θ against x in Fig. 8. The result of this analysis is given in Fig. 9, which shows that in the fully turbulent region the low speed values of A and B (5.5 and 5.75) provide a fairly good fit with the experimental points if density and viscosity in equation (14) are evaluated at wall (plate) temperature instead of at free stream temperature, i.e. the velocity profile might be taken as

$$u/u_{\tau_w} = 5.5 + 5.75 \log_{10} y_{\tau_w} \qquad \ldots\ldots\ldots \quad (15)$$

where

$$u_{\tau_w} = (\tau_o/\rho_w)^{\frac{1}{2}}$$

$$y_{\tau_w} = \frac{y u_{\tau_w}}{\nu_w}$$

and subscript "w" refers to wall temperature conditions. (Fig. 9 also shows that there are no experimental points inboard of a value of y_{τ_1}, corresponding approximately to $y_{\tau_w} = 30$, when $M_1 = 2.46$. In low speed flow, $y_\tau = 30$ is a convenient mark for the inner limit of the "turbulent core" of the boundary layer (see Ref. 5) so that if the extension to compressible flow suggested by equation (15) is valid, then the present results provide no check on the inner layers where viscosity is of importance).

If, lacking data covering a range of Mach numbers and heat transfer conditions, we assume that equation (15) is the general expression for the velocity distribution in the compressible turbulent boundary layer, we can deduce certain results for the variation of skin friction etc., with Mach number and heat transfer. A mathematical analysis is made in Appendix II, based on the following assumptions,

(1) that the velocity profile in the compressible turbulent boundary layer, with or without heat transfer, is given by equation (15), and

(2) that Reynolds analogy between momentum and heat exchange is valid.

It gives the following results, for flows with or without heat transfer and assuming that the layer is turbulent from the leading edge.

(a) Mean skin friction coefficient

Denoting incompressible values by subscript "i" and taking

$$C_{F_w} = \frac{F}{\frac{1}{2} \rho_w u_1^2 x}$$

where F is the skin friction force on length x of plate and

$$Re_w = \frac{u_1 x}{\nu_w}$$

then

$$\left.\begin{aligned} C_{F_i} &= C_{F_w} \\ \text{when} \quad Re_i &= Re_w \, {}^{T_1}/_{T_w} \end{aligned}\right\} \quad \ldots\ldots\ldots\ldots \quad (17)$$

where T_1 is the free stream "static" temperature

and T_w is the wall (plate) temperature.

(The same result is valid for the local skin friction coefficient c_f.)

In the zero heat transfer case, if we assume in accordance with Reynolds analogy that $T_w = T_0$, then use of equation (17) with Schoenherr's formula for low speed skin friction gives the same result as an earlier formula obtained by Cope from the same assumptions. He also takes $\mu \propto T^{\frac{3}{4}}$.

(b) Displacement thickness

Again, if

$$\left.\begin{aligned} Re_i &= Re_w \, {}^{T_1}/_{T_w} \\ \text{then} \quad \frac{\left(\dfrac{\delta^x u_1}{\nu_w}\right)}{\left(\dfrac{\delta^x{}_i u_1}{\nu_i}\right)} &= \frac{T_w}{T_1} + \frac{1}{5} M_1^2 \end{aligned}\right\} \quad \ldots\ldots\ldots \quad (18)$$

(c) Ratio of displacement to momentum thickness

If

$$H = \delta^x/\theta$$

then

$$H/H_i = \frac{T_w}{T_1} + \frac{1}{5} M_1^2 \quad \ldots\ldots\ldots\ldots \quad (19)$$

The present results provide a check on the assumptions behind the above formulae in the zero heat transfer case at $M_1 = 2.46$. For the incompressible skin friction coefficient we shall take Prandtl's formula (see for example, Ref.5)

$$C_{F_i} = 0.46 \, (\log_{10} Re_i)^{-2.6} \quad \ldots\ldots\ldots\ldots \quad (20)$$

which is valid for Re_1 between 10^6 and 10^9 on smooth plates. Then, from equation (17) we obtain the general formula

$$C_{F_W} = 0.46 \left(\log_{10} Re_w \, {}^{T_1}/_{T_w}\right)^{-2.6} \qquad \ldots\ldots (21)$$

The variation of C_F with Re obtained from this formula for zero heat transfer at $M_1 = 2.46$, is compared with the present experimental values ($C_F = {}^{2\theta}/_{x}$) in Fig. 10. The value of ${}^{T_1}/T_w$ for zero heat transfer at $M_1 = 2.46$ (for substitution in equation (21)) was obtained from the empirical formula

$$\frac{T_w}{T_1} = 1 + 0.88 \, \frac{\gamma-1}{2} \, M_1^{\,2} \qquad \ldots\ldots (22)$$

of Ref. 1, in preference to taking $T_w = T_0$ as would be given by Reynolds analogy, since equation (22) corresponds to the experimental conditions. The ratio ${}^{\mu_w}/\mu_1$ was obtained from Sutherland's formula. At high Reynolds numbers, equation (21) and the experimental values are in good agreement with each other.

In obtaining the experimental values of C_F from the formula

$$C_F = {}^{2\theta}/x,$$

"x" was taken as the distance from the leading edge of the plate so that the influence of the laminar portion of the layer is perceptible until high Reynolds numbers are reached. One method of allowing for its effect is to derive C_F from the formula

$$C_F{}' = \frac{2\theta}{x-x_0}$$

and to base Reynolds number on the length $(x-x_0)$ where

$$x = x_0$$

is the position of the effective start of the turbulent layer. If so, then equation (21) becomes

$$C_{F_W} = 0.46 \left(1 - \frac{x_0}{x}\right) \left\{\log_{10} Re_w \, \frac{T_1}{T_w} \left(1 - \frac{x_0}{x}\right)\right\}^{-2.6} \qquad \ldots.(21a)$$

The "transition curve" of C_F against Re obtained from equation (21a) for

$$x_0 = 1.0$$

is shown in Fig. 10. This is the value of x_0 given by Figs. 7 and 8, and in Fig. 10 it gives reasonable agreement with experiment over the whole of the turbulent region. (It should be noted that 0.1 inches on the vertical scale corresponds to an error of approximately 2.5%).

Also shown in Fig. 10 are the incompressible ($M = 0$) variation (equation 20), with density and viscosity evaluated at free stream temperature, which is 40% higher than experiment; and the estimate obtained from Von Karman's suggestion that the incompressible formula be retained but that density and viscosity be evaluated at wall temperature. The latter gives results 15% below the experimental results. Finally, the mean of the preliminary results of Ref. 1 is 20% above the present results.

Considering next the ratio of displacement to momentum thickness, we obtain from equations (19) and (22)

$$H/H_1 = 1 + 0.376\,M_1^2 \qquad \ldots\ldots\ldots \quad (23)$$

$$= 3.275 \text{ at } M_1 = 2.46$$

Taking $H_1 = 9/7$

this gives $H = 4.21$

and this value is compared in Fig. 11 with the experimental values and with the value

$$H = 4.00$$

obtained from Ref. 4 for the 1/7th power law profile. The latter value gives the better mean to the experimental turbulent results and suggests that a change of constant in equation (23) might be desirable. In fact

$$H/H_1 = 1 + 0.35\,M_1^2 \qquad \ldots\ldots\ldots \quad (24)$$

gives good agreement with the 1/7th power law variation for $M < 4$ as is shown by the following table.

	M	1	2	3	4
$\frac{H}{H_1}$	$1 + 0.376\,M_1^2$	1.376	2.504	4.385	7.02
	Ref.4	1.350	2.390	4.170	6.85
	$1 + 0.35\,M_1^2$	1.350	2.400	4.150	6.60

In conclusion therefore, the formula

$$C_{F_w} = 0.46\left(\log_{10} Re_w \, {}^{T_1}/_{T_w}\right)^{-2.6} \qquad \ldots\ldots\ldots \quad (21)$$

is supported by the present experimental results, and they indicate that in the zero heat transfer condition.

$$H/H_i = 1 + 0.35\ M_1^2 \qquad \ldots\ldots\ldots\ (24)$$

with $$H_i = 9/7$$

Further work is obviously necessary, both at other Mach numbers and for cases with heat transfer.

7 Conclusions

Tests made with the experimental apparatus of Ref.1 on an unheated wooden plate under zero heat transfer conditions at a nominal tunnel Mach number of 2.5 show that

(1) By raising the plate 0.16 inches, fitting a sharp edged forward facing lip on to its leading edge and by enlarging the suction slot and piping from the Ref.1 design, it is possible to remove from the leading edge a sufficient proportion of the tunnel wall boundary layer to ensure that the residue has at least 98-99% of the free stream velocity (Figs.1 and 2).

After this has been done

(2) The mean Mach number over the plate is 2.46. The mean Reynolds number, based on free stream conditions and a length of one inch, is 2.5×10^5.

(3) Pitot traverses show that there is a laminar boundary layer over the forward portion of the plate and transition to turbulence occurs between 3 and 4 inches from the leading edge, i.e. at a Reynolds number between 8×10^5 and 10^6. This checks with the result of a chemical indication test.

(4) The accuracy of the pitot traverses was checked by making tests with two different sizes of tube. No effect of tube size was found until they were touching the wall (Fig.12).

(5) The measured rate of growth of thickness, displacement thickness and momentum thickness of the laminar boundary layer are all greater than theory would predict (Figs.5, 7 and 8). However, later experiments (not reported here) indicate that the characteristics of the laminar layer are very dependent on the condition of the knife edge and its exact setting (in height) in relation to the flow through the suction slot. For this reason the present results are to be treated with reserve.

(6) The turbulent boundary layer has not been found to be sensitive to small changes in the leading edge conditions. The velocity profiles are in good agreement with the 1/7th power law profile (Fig.6). Scaling up displacement and momentum thicknesses with the aid of this law gives the boundary layer thickness

$$\delta = 0.378\ Re_X^{-1/5}\ X$$

where X is the distance from the effective start of the turbulent layer (1 inch behind the leading edge, Figs. 7 and 8). This compares with the low speed value

$$\delta = 0.37\ Re_X^{-1/5}\ X\ .$$

Thus there seems to be little change in turbulent boundary layer thickness with Mach number.

(7) In low speed flow, the power law velocity profiles are only approximations to a more general log law turbulent profile of the form

$$u/u_\tau = A + B \log_{10} y_\tau$$

where

$$u_\tau = (\tau_0/\rho)^{\frac{1}{2}}$$

$$y_\tau = \frac{y u_\tau}{\nu}$$

A and B are empirical constants.

The best agreement with low speed experimental results over a wide range of Reynolds numbers has been found5 with A = 5.5 and B = 5.75. (The results are mainly for pipe flows.)

The same values of A and B can be used to give reasonable agreement with the present results for the turbulent layer if density and viscosity are evaluated at wall temperature, i.e. the experimental results lie near the curve

$$u/u_{\tau_w} = 5.5 + 5.75 \log_{10} y_{\tau_w}$$

where subscript "w" refers to wall conditions (Fig.9).

(8) If it were assumed that conclusion (7) was an exact result of general validity (with or without heat transfer) and that Reynolds analogy between momentum and heat exchange is valid, then the variation of skin friction coefficient with Mach number and heat transfer would be given by

$$C_{F_i} = C_{F_w}$$

when

$$Re_i = Re_w \, {}^{T_1}/T_w$$

where subscript "i" denotes the incompressible value

T_1 is the free stream "static" temperature

and T_w is the wall temperature (both in degrees absolute)

(9) A check on the errors involved in the assumptions of conclusion (8) is given by the present skin friction results (obtained from the formula $C_F = 2\theta/x$), for $M_1 = 2.46$ and zero heat transfer. The formula taken for C_{F_i} was

$$C_{F_i} = 0.46 \, (\log_{10} Re_i)^{-2.6}$$

which leads, in accordance with conclusion (8) to

$$C_{F_w} = 0.46 \, (\log_{10} Re_w \, {}^{T_1}/T_w)^{-2.6}$$

The latter formula gives good agreement with the experimental results, (Fig.10) and therefore justifies the assumptions of conclusion (8) in this instance.

(10) The present results for mean skin friction are about 20% below the mean of the preliminary results of Ref.1.

(11) Also derived from the assumptions used in conclusion (8) is the formula

$$H/H_i = {}^{T_W}/_{T_1} + {}^1/_5\, M_1{}^2$$

for the variation of $H = \delta^x/\theta$.

Under zero heat transfer conditions, Ref.1 gave

$$T_W/T_1 = 1 + 0.88\,\frac{\gamma-1}{2}\,M_1{}^2$$

so that in these conditions

$$H/H_i = 1 + 0.376\,M_1{}^2 .$$

However, taking $H_i = 9/7$, the present measurements indicate that the constant should be changed and the equation read

$$H/H_i = 1 + 0.35\,M_1{}^2 .$$

(12) Further checks on the validity of conclusions (8) and (11) are needed, both at other Mach numbers and for cases with heat transfer.

LIST OF SYMBOLS

x	distance along plate from leading edge
y	distance normal to plate
u	velocity at a point in the boundary layer
u_1	free stream velocity (outside boundary layer)
T	temperature at a point in the boundary layer
T_1	free stream temperature
T_o	free stream stagnation temperature
T_w	temperature of wall
ρ	density (subscripts as for temperature)
ν	kinematic viscosity (subscripts as for temperature)
Re, Re_x	Reynolds number based on length x, with free stream wiscosity and velocity
Re_w	Reynolds number based on length x, free stream velocity but viscosity evaluated at wall temperature
δ	thickness of boundary layer
δ^x	displacement thickness of boundary layer $= \int_0^\delta \left(1 - \frac{\rho u}{\rho_1 u_1}\right) dy$
θ	momentum thickness of boundary layer $= \int_0^\delta \frac{\rho u}{\rho_1 u_1} (1 - {}^u/u_1)\, dy$
τ_o	local skin friction
F	total skin friction on length x, $= \int_0^x \tau_o \, dx$
c_f	local skin friction coefficient $= \frac{\tau_o}{\frac{1}{2} \rho_1 u_1^2} = 2 \frac{d\theta}{dx}$ if no pressure gradient
C_F	mean skin friction coefficient $= \frac{F}{\frac{1}{2} \rho_1 u_1^2 x} = 2 \frac{\theta}{x}$ if no pressure gradient

LIST OF SYMBOLS (Contd.)

$$C_{F_w} = \frac{F}{\frac{1}{2}\rho_w u_1^2 x}$$

$$u_\tau = \left({}^{\tau_o}/_{\rho}\right)^{\frac{1}{2}}$$

$$u_{\tau_w} = \left({}^{\tau_o}/_{\rho_w}\right)^{\frac{1}{2}}$$

$$y_\tau = \frac{yu_\tau}{\nu}$$

$$y_{\tau_w} = \frac{yu_{\tau_w}}{\nu_w}$$

LIST OF REFERENCES

No.	Author	Title, etc.
1	J.E. Johnson and R.J. Monaghan	The measurement of heat transfer and skin friction at supersonic speeds. Preliminary results of measurements on a flat plate at a Mach number of 2.5. Current Paper No. 59. April, 1949.
2	J. Lukasiewicz and J.K. Royle	Boundary layer and wake observation in supersonic flow. R & M 2613. Oct. 1948.
3	R.J. Monaghan	An approximate solution of the compressible laminar boundary layer on a flat plate. R & M 2760. Nov. 1949.
4	W.F. Cope and G.G. Watson	Preliminary measurements of the boundary layer in the 11" supersonic tunnel. R & M 2304. Aug. 1946.
5	Edited by S. Goldstein	Modern developments in fluid dynamics. Vol. II. Clarendon Press, Oxford. 1938.

APPENDIX I

Chemical Indication of Transition

Analysis of the pitot traverse measurements showed that transition from laminar to turbulent flow was taking place between three and four inches from the leading edge, but the shape of the transition front across the plate was not known. It was therefore decided to experiment with chemical indicators to see what results could be obtained under supersonic tunnel conditions.

Both evaporation and contamination methods were considered. For the first, the plate would be sprayed with a thin coating of some slightly volatile compound before assembly in the tunnel and the differential rate of evaporation of the coating would then distinguish between the laminar and turbulent regions. For the second, the chlorine method was chosen for trial, in which the plate would be sprayed with a solution of potassium iodide in starch and, when the correct flow conditions were established, a small amount of chlorine gas would be mixed with the air flowing through the tunnel and the differential rate of contamination of the potassium iodide by the chlorine would indicate the transition front.

Difficulties arose in the application of either method to the supersonic tunnel used in the present tests.

With the evaporation method, a compound has to be selected having a very low volatility as the plate has to be sprayed before assembly of the tunnel, which, with the present rig, takes about two hours; following which the correct flow and temperature conditions have to be established. The time to be allowed for the latter is doubtful. It takes about thirty seconds to establish supersonic flow in the working section, during which time there are violent disturbances in the tunnel. It may then take fifteen to thirty minutes to obtain the correct stagnation temperature, but it is possible that, from the point of view of fixing transition, the temperature may be sufficiently close to the correct value after about five to ten minutes. It follows therefore that the compound must have negligible volatility under atmospheric conditions and evaporate fairly slowly under tunnel conditions. Also the coating should be thin so as not to affect the heat transfer from the plate to the stream, but at the same time it should be easily visible through the tunnel windows.

Because of the difficulties inherent in the evaporation method, it might be expected that the chlorine method would be more suitable.. In theory, its chief advantage is that the surface remains inactive while the tunnel is being assembled and started up. Then, when correct conditions have been obtained, the chlorine is introduced and the indication obtained within a few minutes. Also, the coating on the plate can be much thinner than with the evaporation method.

However, the reaction between chlorine and potassium iodide depends on the presence of water vapour in the air, and unfortunately the air in the tunnel has to be relatively dry in order to avoid condensation shocks. As a result, no reaction could be obtained in the first chlorine tests.

To overcome this difficulty, glycerine was added to the potassium iodide solution and this enabled a reaction to occur. The reaction was, however, negative in that the colouring occurred at places on the plate associated with a low rate of shear, whereas the opposite should be the case. It is thought that this occurs because the glycerine may evaporate from the plate while the tunnel airflow is being brought to the steady condition. If so, it would evaporate more from those places with a high rate of shear than from those with a low rate, so that when the chlorine is introduced it is only at the latter places that there is sufficient glycerine left to precipitate the reaction. The chief advantage of the chlorine method is therefore nullified, since it seems that the surface does not remain inactive during the starting process.

It was also found difficult to obtain uniform mixing of the chlorine with the air stream, but this was partly overcome by introducing the chlorine into the duct well upstream of the tunnel.

The evaporation method was then tried. Dr. Main-Smith of Chemistry Dept. supplied a sample of azobenzene, which was sprayed on to the plate as a solution in light petroleum. This dried, leaving an orange coloured crystalline film. It was found that a thick coating gave the best results, but the length of time of exposure to the airstream was somewhat indeterminate, varying from $\frac{3}{4}$ to 3 hours. Initially tests were made with a white cellulose finish on the plate but latterly a black pheno-glaze finish was used.

Fig.13 shows the result obtained with azobenzene on the black-finished plate after an exposure of 1 hour 20 minutes to the airflow. It is not a good picture for defining transition, since there is no sharply defined border to the (white) laminar region at the front of the plate, apart from the disturbances from the corners which spread inwards to meet at a point about six inches from the leading edge. The uneven evaporation from the plate may arise from the difficulty of securing a uniform thick coating. The probable transverse line of transition, as deduced from the pitot traverses, has been added.

Of interest are the disturbances from the pitot tube and support. A pitot traverse was made during the test and the pitot tube was held for finite lengths of time at different heights from the surface, which explains the number of discrete intersections of the disturbances with the plate. Behind these shock wave intersections there is very little evaporation, which suggests either that there is separation or that the boundary layer has been thickened to such an extent that the shearing stress is very low.

This test was made with a plate temperature of about plus 17 deg.C. In a later test, made with a plate temperature of about minus 25 deg.C and with a thinner coating of azobenzene, no evaporation took place even after three hours running time. Pitot measurements showed that transition did take place, so the failure of the chemical method must be ascribed to a temperature effect on the azobenzene.

The existence of this temperature effect is serious where the present series of experiments is concerned, because boundary layer measurements will be required over a range of plate temperatures up to plus 100 deg.C.

The results of this preliminary investigation are therefore:

(1) The contamination method is a priori the more suitable in the present instance but substances must be found whose reaction does not depend on the presence of water vapour in the airstream.

(2) Moderate success was obtained from the evaporation method, using azobenzene, but it seems that another compound must be found if it is to be used over a range of plate temperatures.

APPENDIX II

Derivation of formulae for turbulent skin friction, etc.

It is assumed that the velocity profile in the compressible turbulent boundary layer on a flat plate, with or without heat transfer is given by

$$u/u_{\tau_w} = 5.5 + 5.75 \log_{10} y_{\tau_w}$$

$$= 5.5 + {}^1/k \ln y_{\tau_w} \qquad \ldots\ldots\ldots \text{II.1}$$

where

$$\ln = \log_e$$

$$k = 0.400$$

$$u_{\tau_w}^2 = \tau_o/\rho_w,$$

$$y_{\tau_w} = \frac{y\, u_{\tau_w}}{\nu_w}$$

and subscript "w" denotes that density and viscosity are evaluated at wall temperature.

It is also assumed that Reynolds analogy between momentum and heat exchange is valid. If so, then the temperature distribution in the layer is given by

$$T/T_w = 1 - \beta\, u/u_1 - \alpha\,(u/u_1)^2 \qquad \ldots\ldots\ldots \text{II.2}$$

where

$$\beta = 1 - T_o/T_w \qquad \ldots\ldots\ldots \text{II.3}$$

$$\alpha = \frac{T_o}{T_w} \cdot \frac{M_1^2}{M_1^2 + 5} \qquad \ldots\ldots\ldots \text{II.4}$$

and T_o is the free stream stagnation temperature. (It is assumed that $\gamma = 1.4$.)

(Note that zero heat transfer at the wall corresponds to $T_w = T_o$ by Reynolds analogy, whereas Ref.1 gives $T_w = 1.07T_o$ at $M_1 = 2.5$ and zero heat transfer. Thus equation II.2 is slightly in error.)

Skin Friction

The local skin friction (τ_o) at a point (x) on the wall is given by

$$\tau_o = \frac{d}{dx} \int_0^{\delta} \rho u\,(u_1 - u)\, dy \qquad \ldots\ldots \text{II.5}$$

Now equation II.1 can be written in the form

$$y = a \frac{\nu_w}{u_{\tau_w}} \exp \left\{ k \, {}^{u}/{u_{\tau_w}} \right\} \qquad \text{II.6}$$

where

$$a = 0.111 \qquad \text{II.7}$$

Put $z = {}^{u}/{u_1}$ and $v = {}^{u_1}/{u_{\tau_w}} = \left(\frac{2}{c_{f_w}} \right)^{\frac{1}{2}}$ then II.6 becomes

$$y = a \frac{\nu_w v}{u_1} \exp. \, (kvz)$$

hence

$$dy = a \, kv^2 \, \frac{\nu_w}{u_1} \left\{ \exp \, (kvz) \right\} dz \qquad \text{II.8}$$

Also, equation II.2 becomes

$$ {}^{T}/{T_w} = 1 - \beta z - \alpha z^2 \qquad \text{II.9}$$

and since the static pressure (p) is constant across the layer we have

$$ {}^{\rho}/{\rho_w} = {}^{T_w}/{T} \qquad \text{II.10}$$

Then substituting from II.8, II.9 and II.10 in II.5 we have

$$\frac{\tau_o}{\rho_w u_1{}^2} = \frac{a \, k\nu_w}{u_1} \, \frac{d}{dx} \, (v^2 I) \qquad \text{II.11}$$

where

$$I = \int_o^1 \frac{z(1-z) \exp(kvz)}{1 - \beta z - \alpha z^2} \, dz \qquad \text{II.12}$$

or

$$\frac{u_1}{\nu_w} = akv^2 \, \frac{d}{dx} \, (v^2 I) \qquad \text{II.11a}$$

Equation II.12 can be integrated either by expanding the denominator as a power series in z and integrating term by term or by partial integrations. Now v is large and as is customary in evaluating the incompressible case we shall neglect all terms not multiplied by $\exp(kv)$ and retain only the first surviving term of the power series in $1/v^2$. When this is done we obtain

$$I = \frac{\exp(kv)}{k^2v^2(1-\beta-\alpha)} \qquad \ldots\ldots\ \text{II.13}$$

hence equation II.11a becomes

$$\frac{u_1}{\nu_w} = a\,kv^2 \frac{d}{dx}\left\{\frac{\exp(kv)}{k^2(1-\beta-\alpha)}\right\}$$

which by integration from 0 to x becomes

$$\frac{u_1x}{\nu_w} = \frac{av^2\exp(kv)}{k(1-\beta-\alpha)}\left\{1 - \frac{2}{kv} + \frac{2}{k^2v^2}\right\}$$

$$\doteq \frac{av^2\exp(kv)}{k(1-\beta-\alpha)}$$

or

$$Re_{x_w}\,Cf_w = \frac{2a}{k(1-\beta-\alpha)}\exp\left\{k\sqrt{(2/cf_w)}\right\} \qquad \ldots\ldots\ \text{II.14}$$

Now in low speed flow

$$\alpha = \beta = 0$$

and therefore

$$Re_{x_i}\,C_{f_i} = \frac{2a}{k}\exp\left\{k\sqrt{(2/cf_i)}\right\} \qquad \ldots\ldots\ \text{II.15}$$

where subscript "i" denotes the incompressible value.

From equations II.14 and II.15 we then see that if

then
$$\left.\begin{aligned} Cf_i &= Cf_w \\ Re_{x_i} &= Re_{x_w}(1-\beta-\alpha) \\ &= Re_{x_w}\,T_1/T_w \end{aligned}\right\} \qquad \ldots\ldots\ \text{II.16}$$

Also, since

$$F = \int_0^x . \tau_o \, dx$$

we have, from II.11

$$\frac{F}{\frac{1}{2}\rho_w u_1{}^2 x} \; \frac{u_1 x}{\nu_w} = 2a \; k \; v^2 I$$

$$= \frac{2a}{k} \; \frac{\exp(kv)}{1-\beta-\alpha}$$

or

$$C_{F_w} \; Re_w = \frac{2a}{k} \; \frac{\exp\left\{k\sqrt{(2/c_{f_w})}\right\}}{1-\beta-\alpha} \qquad \text{...... II.17}$$

and

$$C_{F_i} \; Re_i = \frac{2a}{k} \; \exp\left\{k\sqrt{(2/c_{f_i})}\right\} \qquad \text{...... II.18}$$

Then from II.16, II.17 and II.18 we see that

$$\left.\begin{aligned} C_{F_i} &= C_{F_w} \\ \text{when} \qquad Re_i &= Re_w \; (1-\beta-\alpha) \\ &= Re_w \; {}^{T1}/T_w \end{aligned}\right\} \qquad \text{...... II.19}$$

Displacement Thickness

The displacement thickness (δ^x) is given by

$$\delta^x = \int_c^\delta \left(1 - \frac{\rho u}{\rho_1 u_1}\right) dy$$

which with the same substitutions as above becomes

$$\frac{\delta^x u_1}{\nu_w} = akv^2 \int_0^1 \left\{1 - \frac{(1-\beta-\alpha)\, z}{1-\beta z-\alpha z^2}\right\} \; e^{kvz} \, dz \qquad \text{... II.20}$$

Then, assuming v to be large and making the same approximations as in the solution of the skin friction equation, II.20 becomes

$$\frac{\delta^x u_1}{\nu_w} = \frac{a}{k} e^{kv} \frac{1+\alpha}{1-\beta-\alpha} \qquad \text{......} \ \text{II.21}$$

In the incompressible case, $\alpha = \beta = 0$ and therefore

$$\frac{\delta^x{}_i u_1}{\nu_i} = \frac{a}{k} e^{kv_i} \qquad \text{.....} \ \text{II.21}$$

It then follows that

$$\left.\begin{aligned} & \frac{\dfrac{\delta^x u_1}{\nu_w}}{\dfrac{\delta^x{}_i u_1}{\nu_i}} = \frac{1+\alpha}{1-\beta-\alpha} \\ & \qquad\qquad = \frac{T_w}{T_1} + \frac{1}{5} M_1{}^2 \\ & \text{if } \quad v = v_i \\ & \text{i.e. if} \qquad Re_{x_i} = Re_{x_w} (1-\beta-\alpha) \\ & \qquad\qquad\quad = Re_{x_w} {}^{T_1}/_{T_w} \end{aligned}\right\} \qquad \text{.....} \ \text{II.22}$$

Ratio of displacement thickness to momentum thickness

In the absence of pressure gradients

$$C_F = {}^{2\theta}/_x$$

hence

$$C_F \, Re_w = 2 \, \frac{\theta u_1}{\nu_w}$$

and equations II.17 and II.18 then show that

$$\frac{\theta u_1}{\nu_w} = \frac{\theta_i u_1}{\nu_i} \quad \text{if} \quad v = v_i \qquad \text{.....} \ \text{II.23}$$

Put

$$\delta^{x}/\theta = H \quad \text{and} \quad \delta^{x}{}_{i}/\theta_{i} = H_{i}$$

then equations II.22 and II.23 show that

$$\frac{H}{H_i} = \frac{T_w}{T_1} + \frac{1}{5} M_1{}^2 \qquad \text{......... II.24}$$

TABLE I

Measurements of boundary layer on dummy hot plate in zero heat transfer condition

Mean M_1 = 2.46 Variation = ± 2%

x = distance downstream from leading edge of plate

x inches	Re_x	δ^x inches	θ inches	$C_F = 2\theta/x$	$H = \frac{\delta^x}{\theta}$
0.82	0.204×10^6	0.0099 0.0111	0.0020 0.0016	0.0049 0.0039	4.95 6.93 [x]
1.90	0.467×10^6 0.475×10^6	0.0162 0.0148	0.0028 0.0025	0.0029_5 0.0026	5.78 5.92
3.0	0.693×10^6	0.0196	0.0035	0.0023	5.60
4.2	1.04×10^6	0.0191	0.0045	0.0021_5	4.24
5.95	1.34×10^6 1.53×10^6	0.0340 0.0303	0.0081 0.0077	0.0027 0.0026	4.20 3.94
10.95	2.66×10^6 2.71×10^6	0.0534 0.0562	0.0139 0.0141	0.0025_5 0.0026	3.84 3 98
13.5	3.44×10^6 3.49×10^6	0.0652 0.0643	0.0163 0.0164	0.0024_2 0.0024_3	4.00 3.92

[x] Two estimates at x = 0.82 made possible by different fairings of the pitot traverse results.

TABLE II

Preliminary results from re-designed tunnel

Mean M_1, in region of measurements, = 2.43

Variation < ± $\frac{3}{4}$%

x inches	Re_x	δ^x inches	θ inches	C_F $= 2\theta/x$	$H = \delta^x/\theta$
3.50	0.834×10^6	0.0210	0.0045	0.00257	4.67
4.25	1.01×10^6	0.0221	0.0055	0.00259	4.02
4.35	1.07×10^6	0.0236	0.0059	0.00271	4.00
6.10	1.42×10^6	0.0320	0.0077	0.00252	4.16
8.19	1.93×10^6	0.0428	0.0107	0.00261	4.00
10.9	2.60×10^6	0.0552	0.0137	0.00251	4.03
13.0	3.17×10^6	0.0647	0.0162	0.00249	4.00

All velocity profiles are fully turbulent.

WT.2078.CP64.K3. Printed in Great Britain.

FIG. 1 a & b.

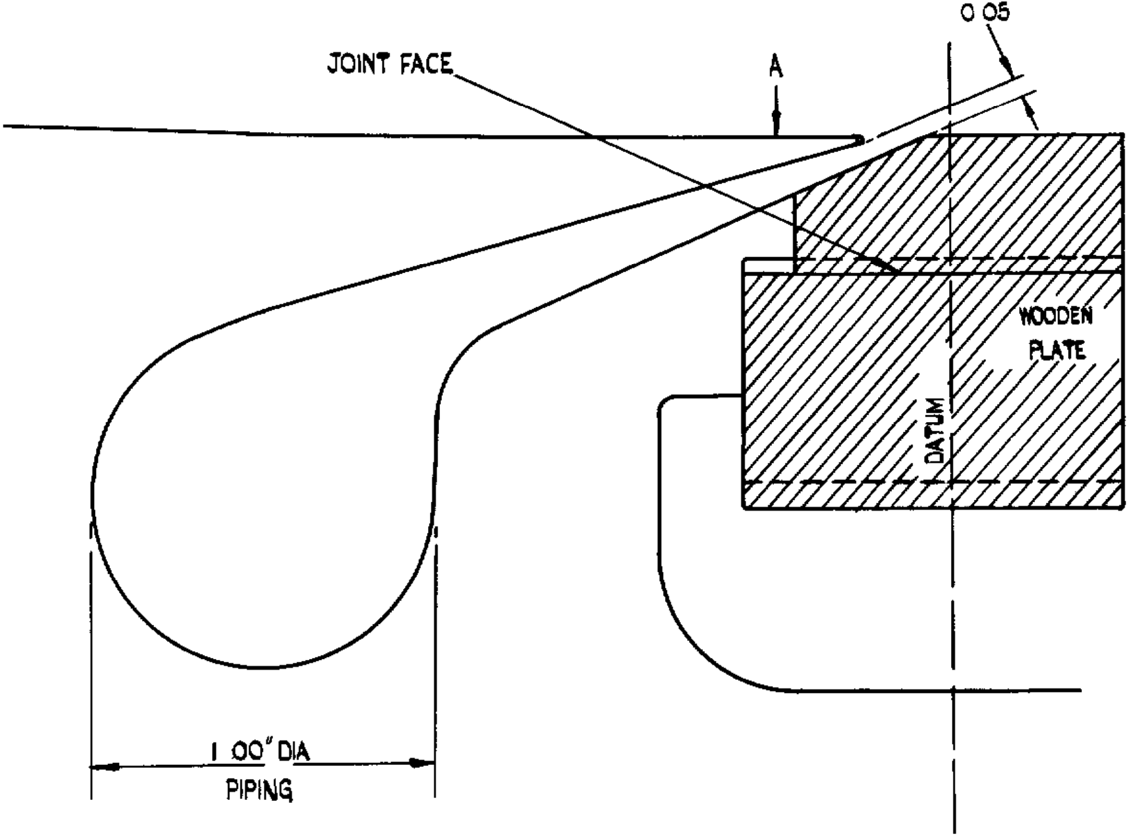
0 05
JOINT FACE
A
WOODEN PLATE
DATUM
1 00" DIA
PIPING

(a) ORIGINAL DESIGN. PLATE SURFACE LEVEL WITH WALL.

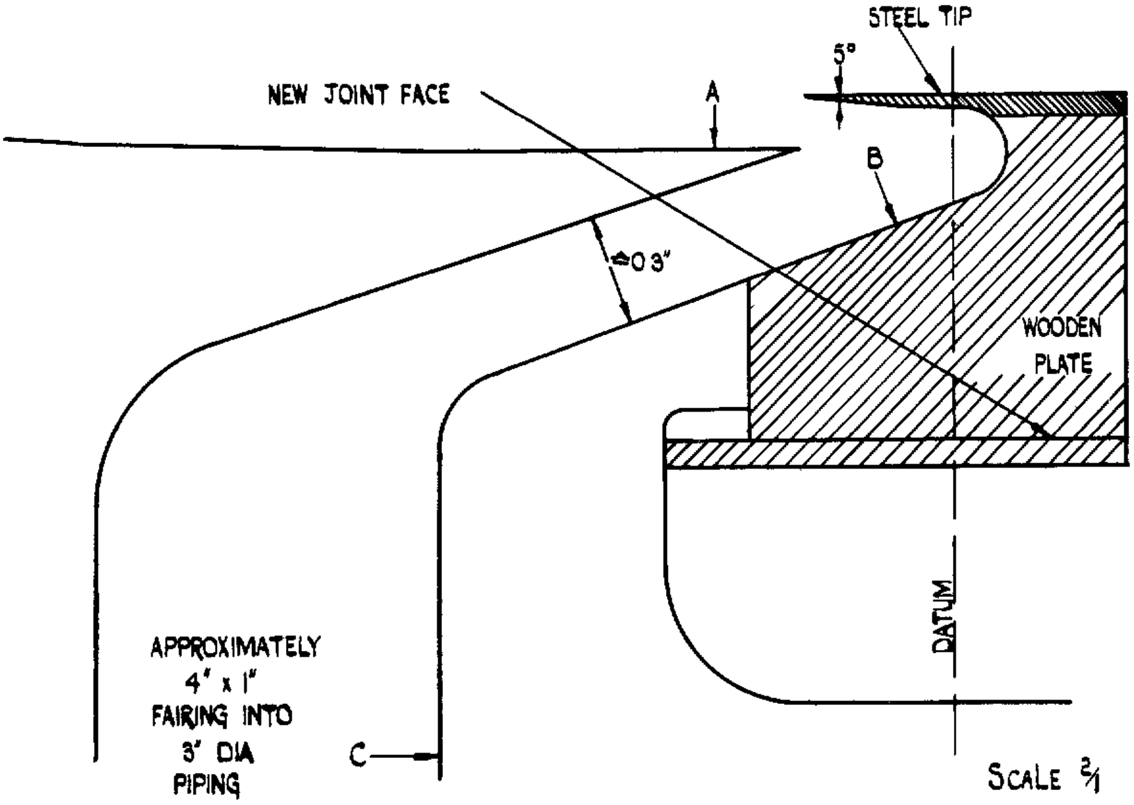
STEEL TIP
5°
NEW JOINT FACE
A
B
≏0 3"
WOODEN PLATE
DATUM
APPROXIMATELY 4" x 1" FAIRING INTO 3" DIA PIPING
C
SCALE 2/1

(b) FINAL MODIFICATION. PLATE RAISED 0·16 INCHES PRESSURES MEASURED AT POINTS "A" "B" AND "C"

FIG. 1 (a & b) MODIFICATION OF SLOT FOR REMOVAL OF TUNNEL BOUNDARY LAYER.

FIG.2.

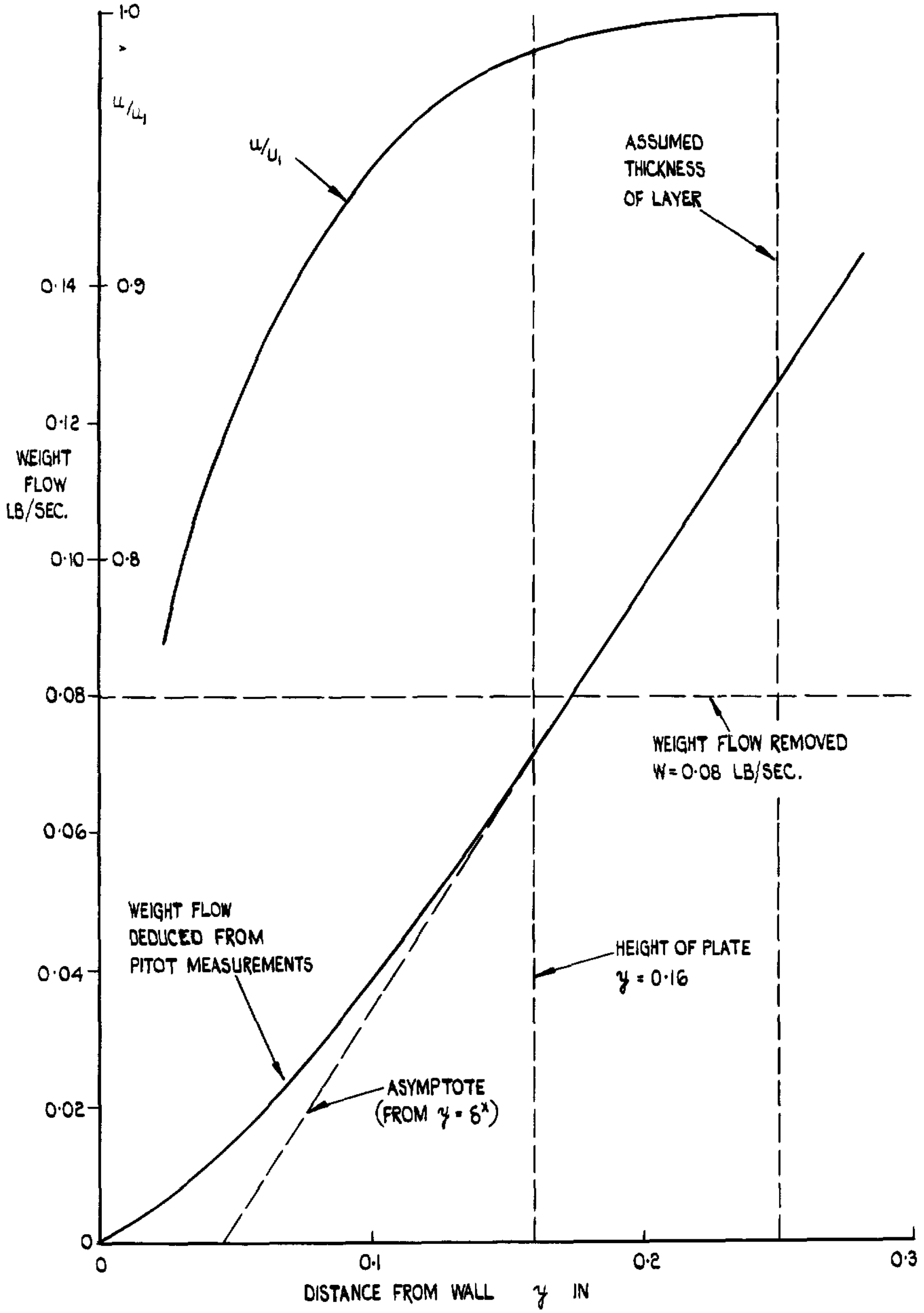

FIG. 2. VELOCITY PROFILE AND WEIGHT FLOW OF AIR IN BOUNDARY LAYER ¼" AHEAD OF SLOT. (POSITION "A" IN FIG. 1.)

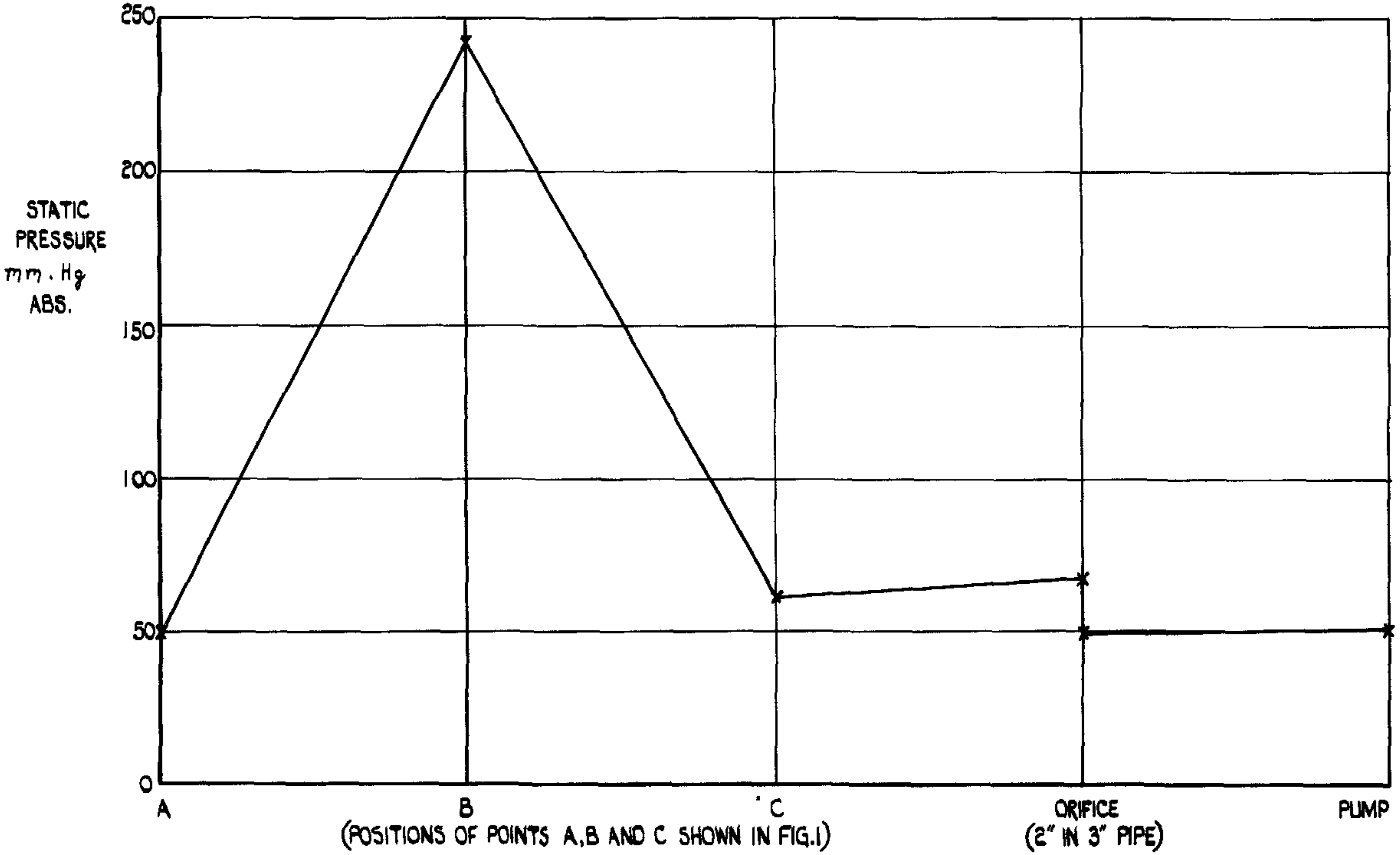

FIG. 3. PRESSURE DISTRIBUTION THROUGH SUCTION SLOT AND PIPE.

FIG.3.

FIG.4 & 5.

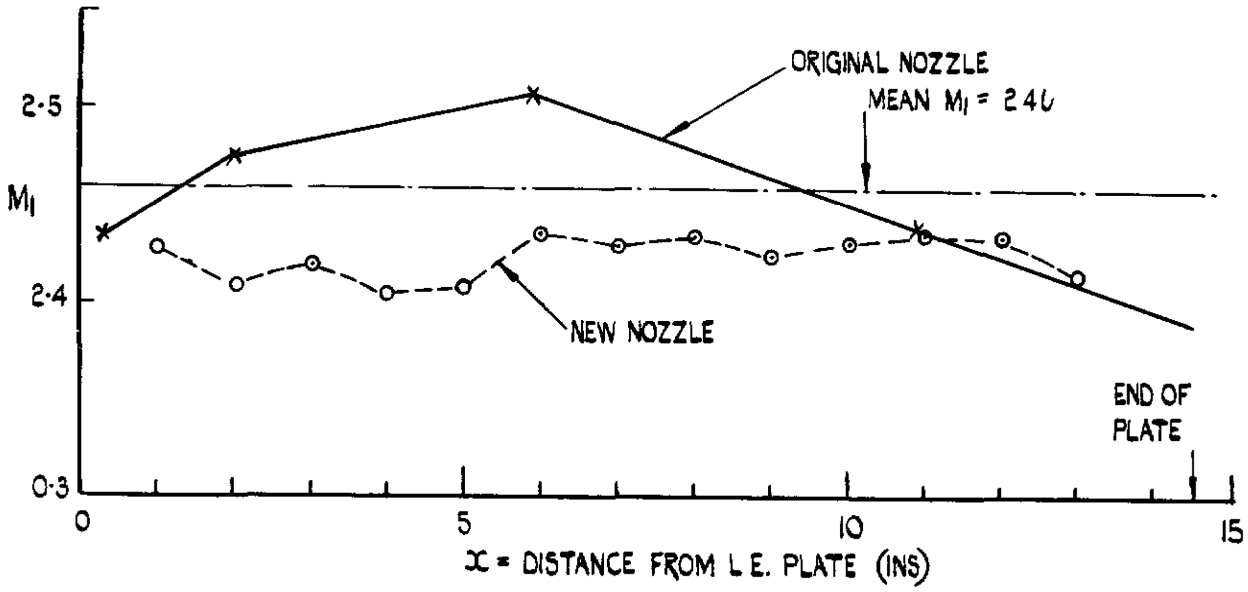

FIG.4. MACH NUMBER VARIATION ALONG PLATE. (OBTAINED FROM WALL STATIC PRESSURES)

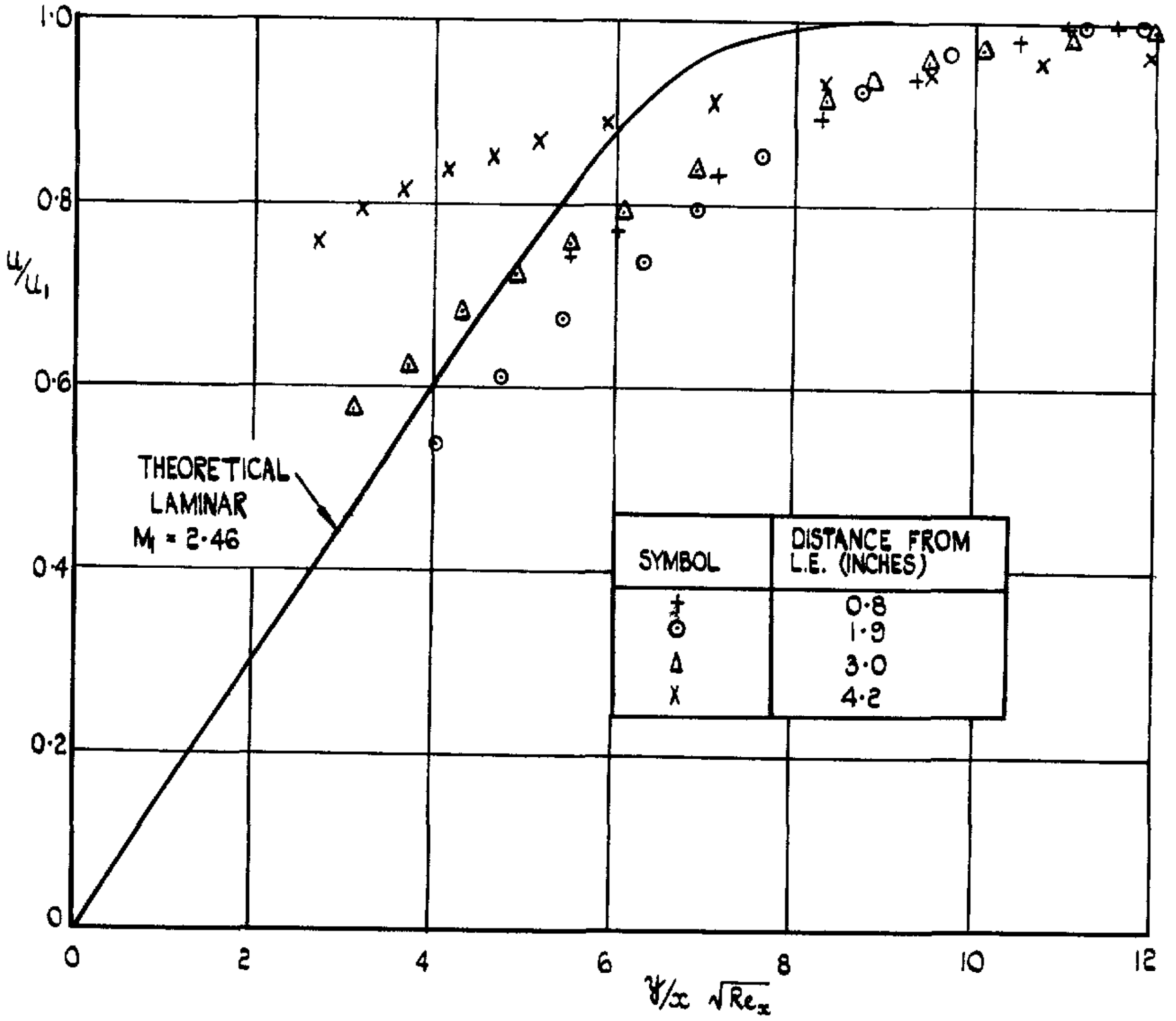

FIG.5. VELOCITY PROFILES IN BOUNDARY LAYER OVER FORWARD PORTION OF PLATE ($x \leqslant 4{\cdot}2''$)

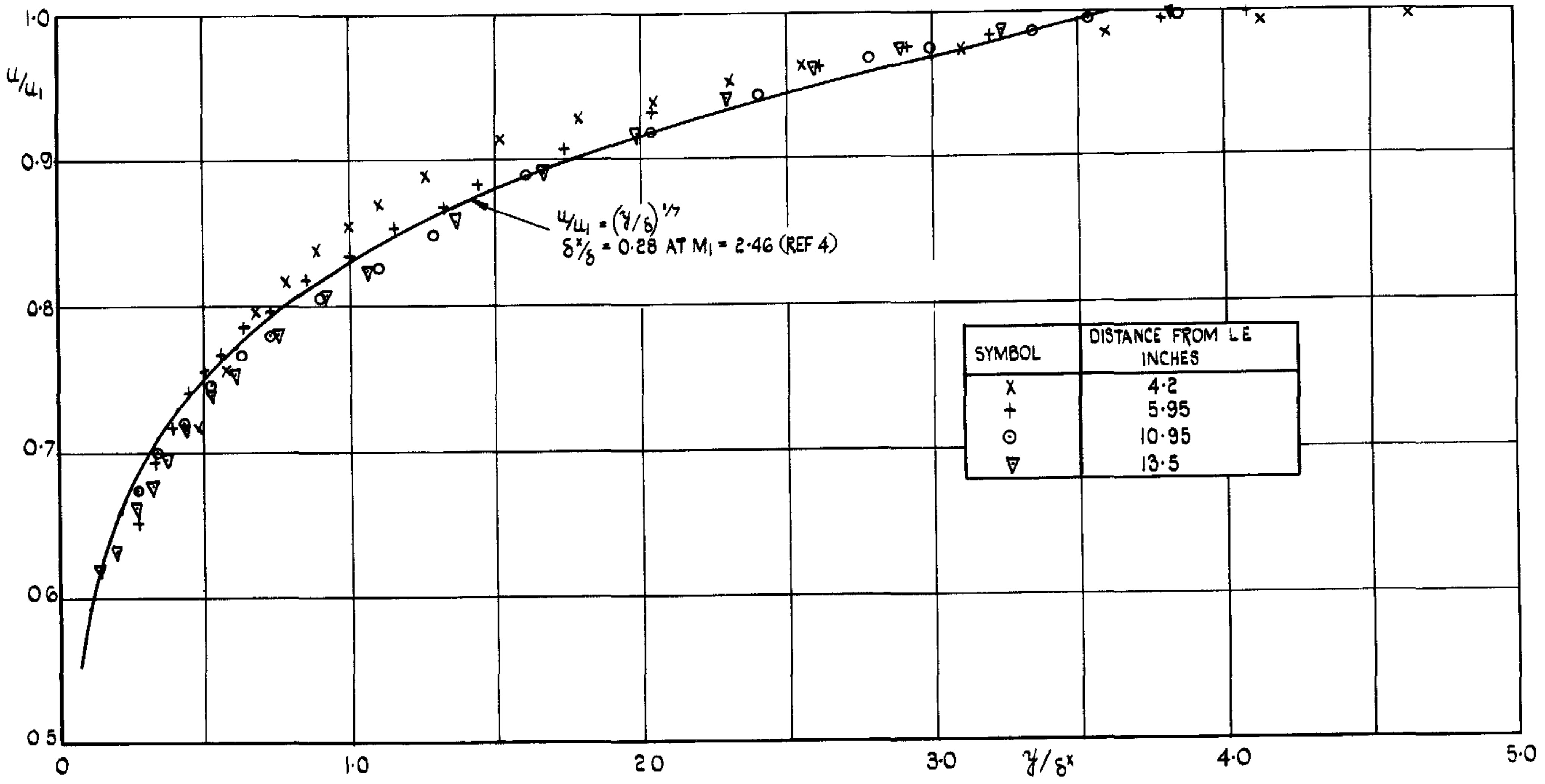

FIG. 6. VELOCITY PROFILES IN BOUNDARY LAYER OVER REAR PORTION OF PLATE $(x > 4'')$

FIG.6.

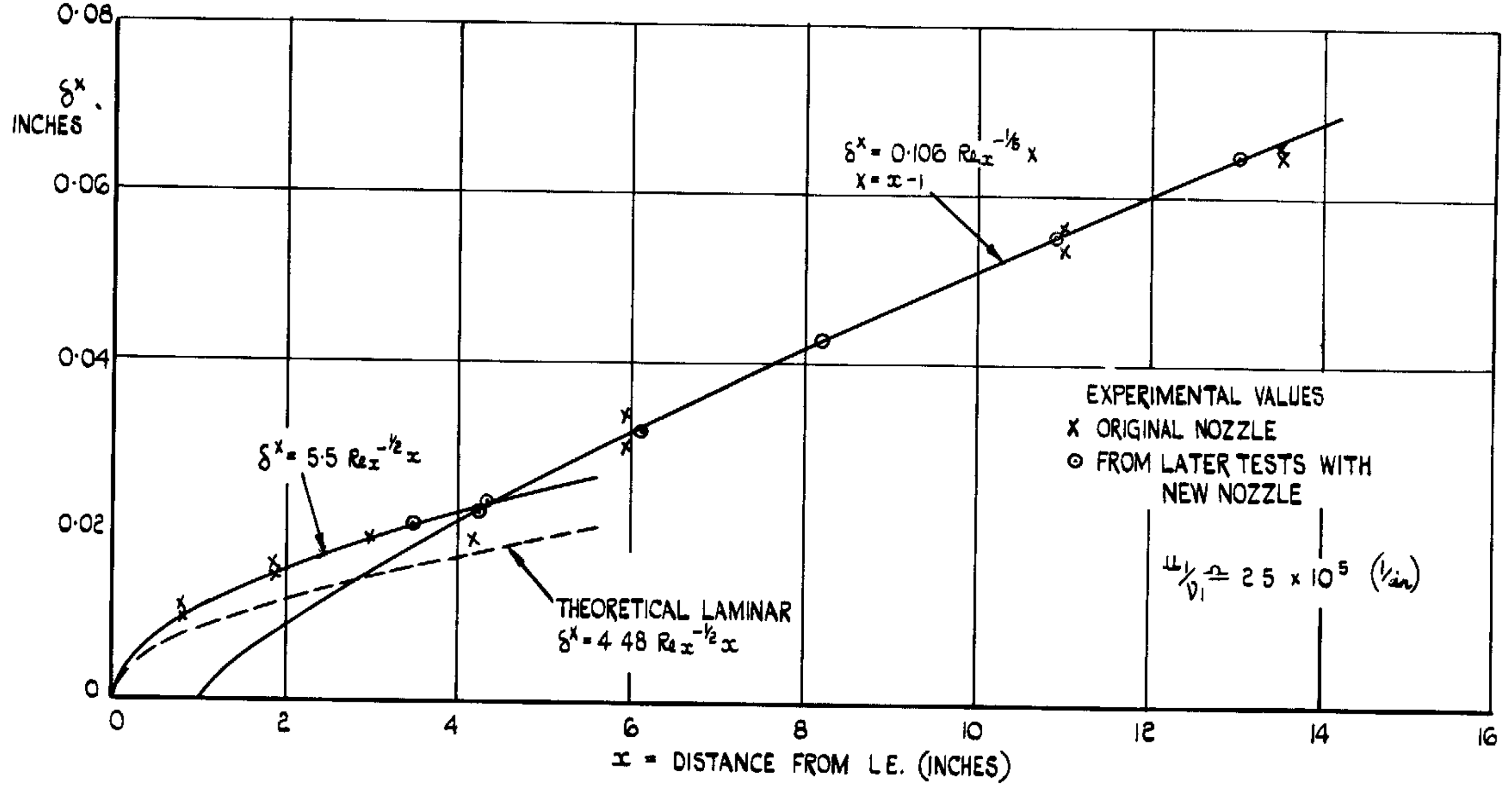

FIG. 7. VARIATION OF DISPLACEMENT THICKNESS ALONG PLATE.

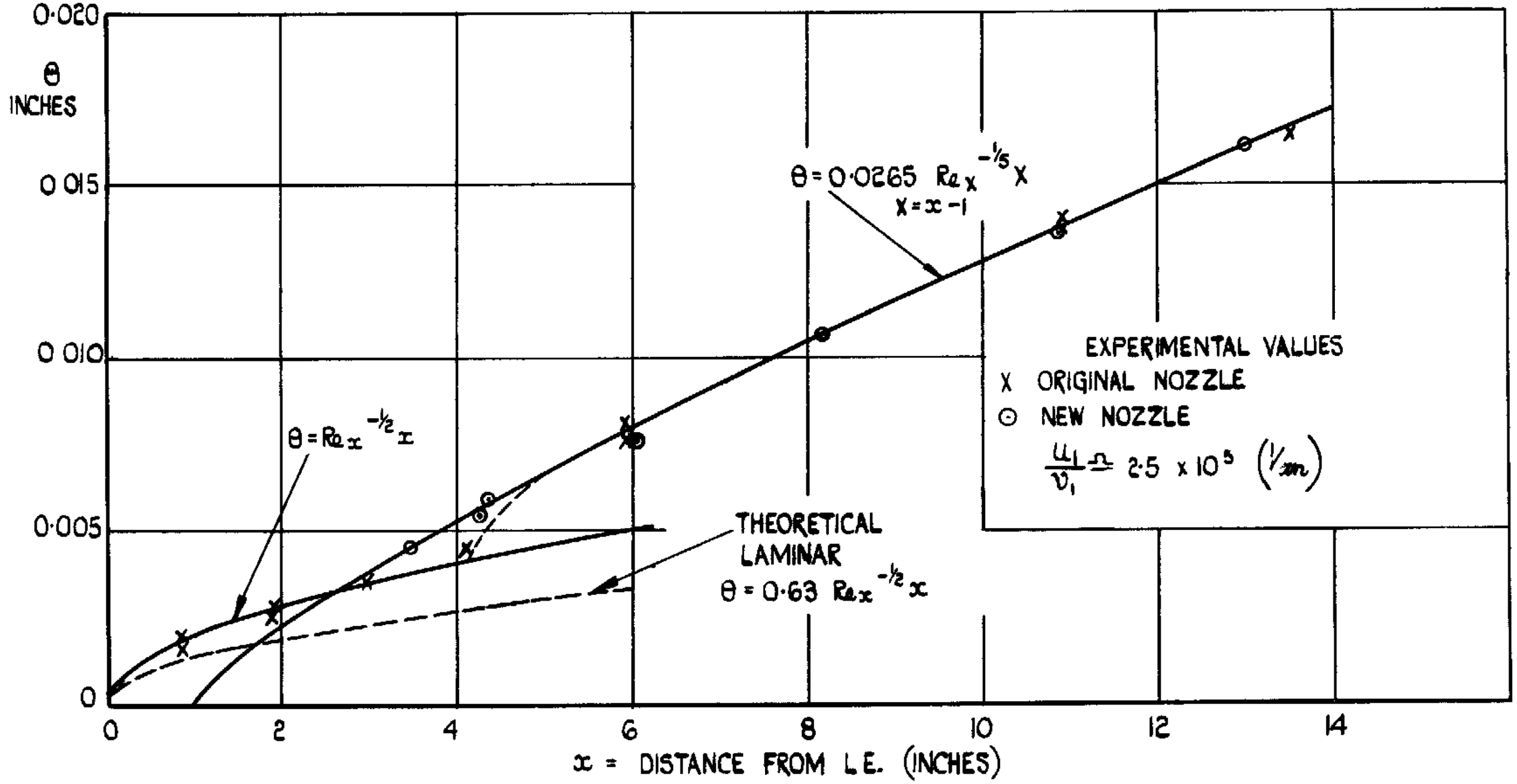

FIG. 8. VARIATION OF MOMENTUM THICKNESS ALONG PLATE.

FIG. 9.

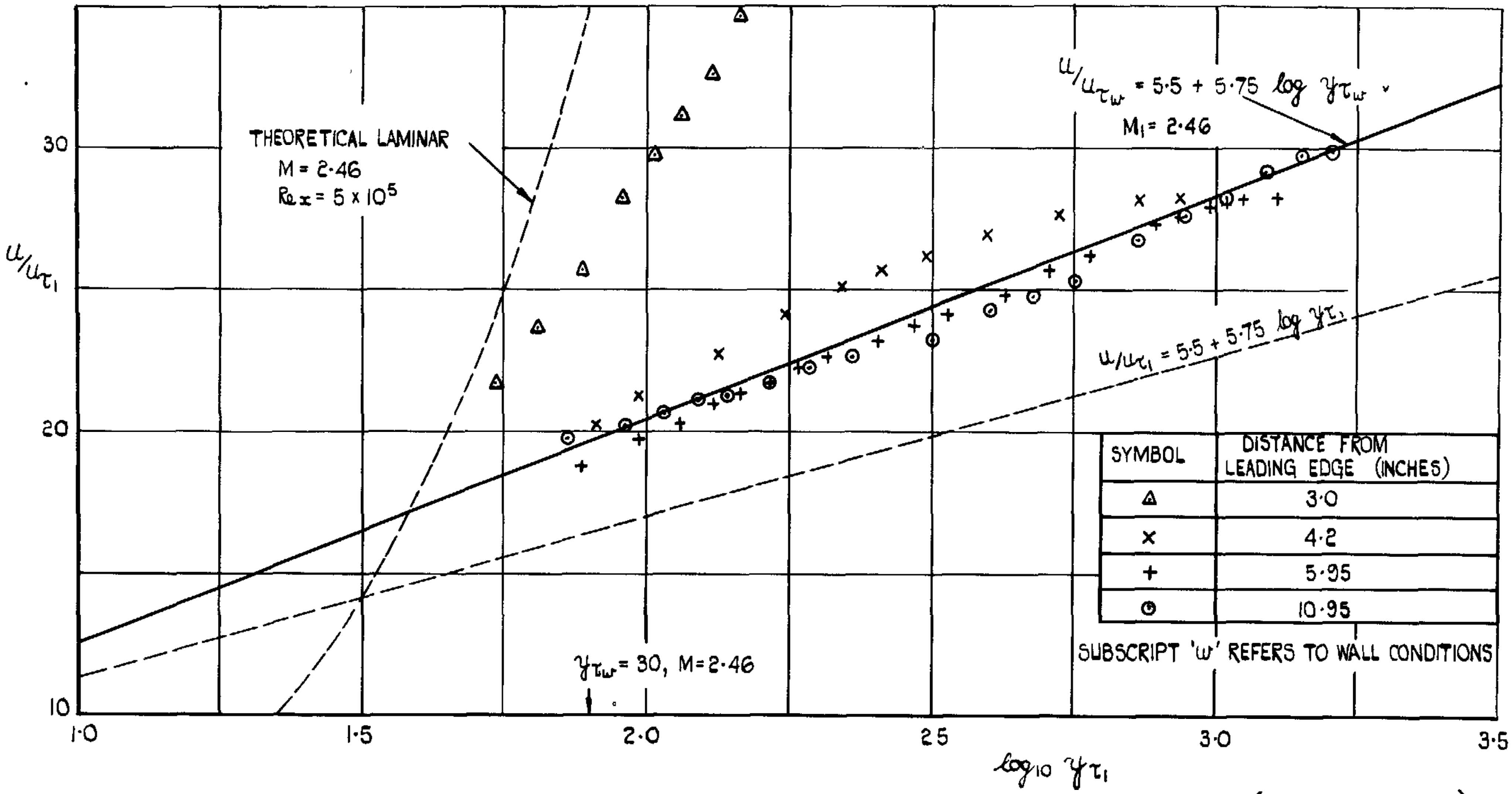

FIG. 9. VELOCITY PROFILES IN BOUNDARY LAYER (LOG LAW.)
(LOCAL SKIN FRICTION ESTIMATED FROM FIG. 8.)

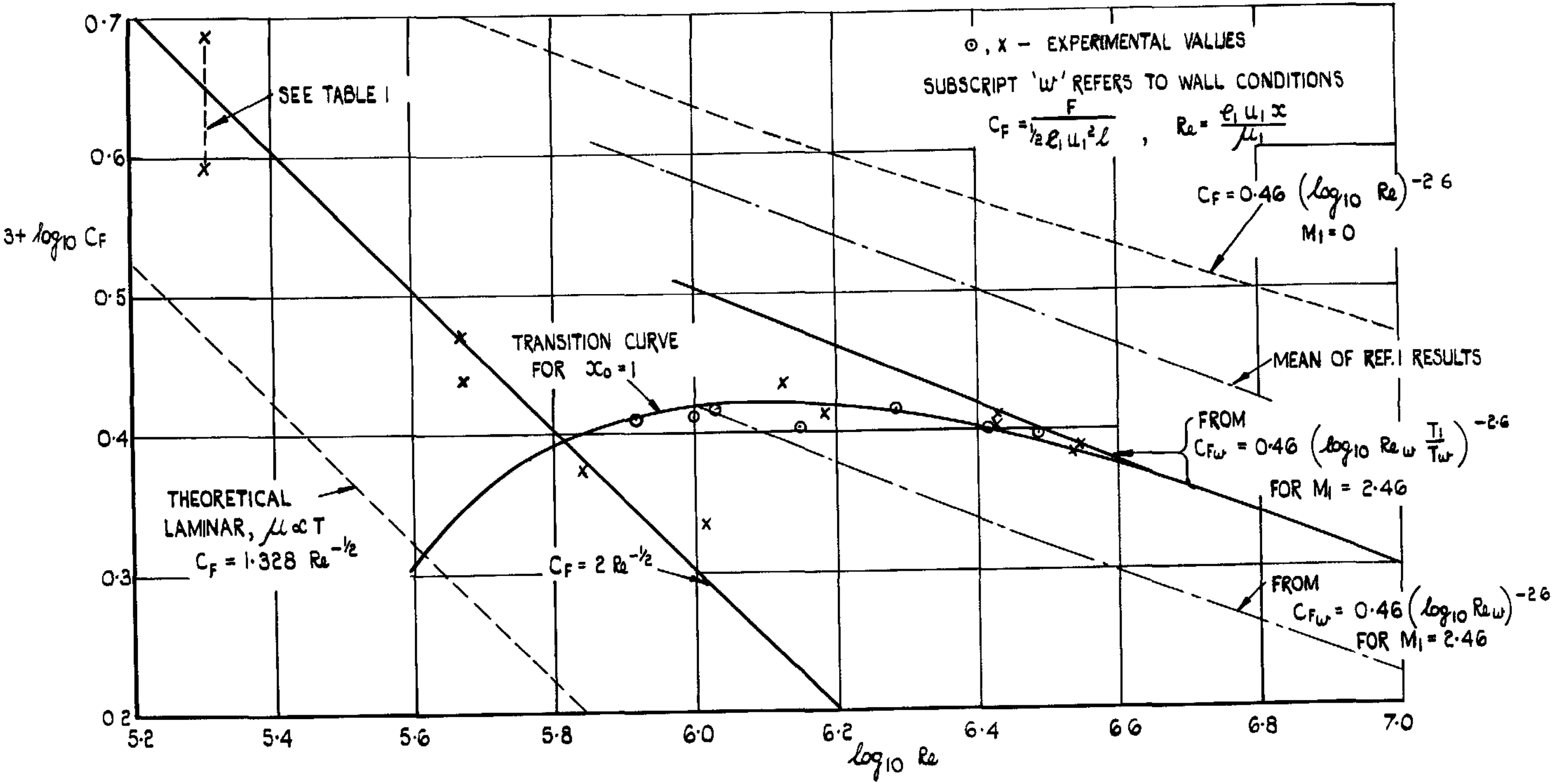

FIG. 10. COMPARISON OF EXPERIMENTAL AND THEORETICAL ESTIMATES OF MEAN SKIN FRICTION COEFFICIENT. AT $M_1 = 2{\cdot}46$ AND ZERO HEAT TRANSFER.

FIG. 10.

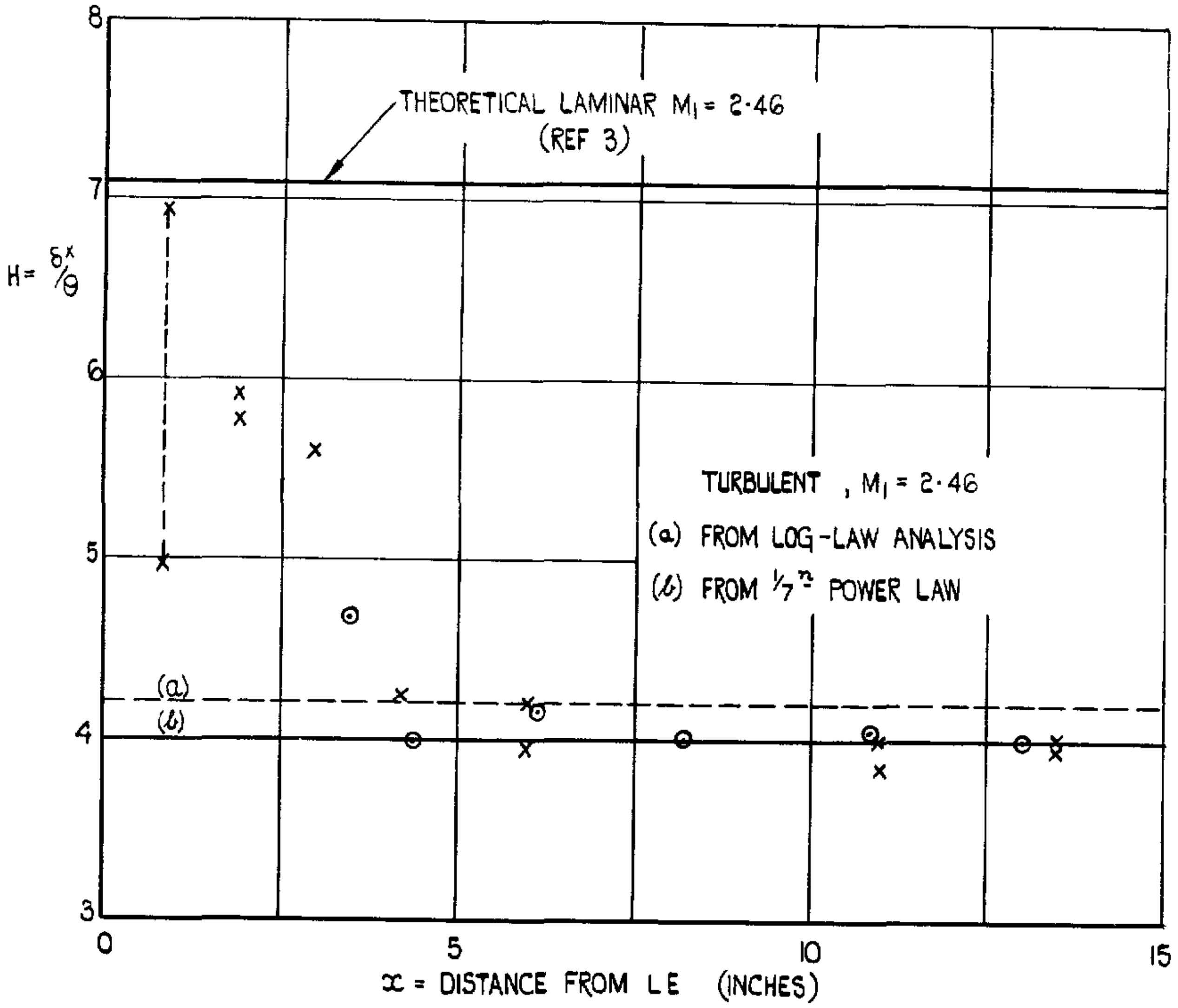

FIG. 11. RATIO OF DISPLACEMENT THICKNESS TO MOMENTUM THICKNESS.
(MEAN $M_1 = 2{\cdot}46$ ZERO HEAT TRANSFER.)

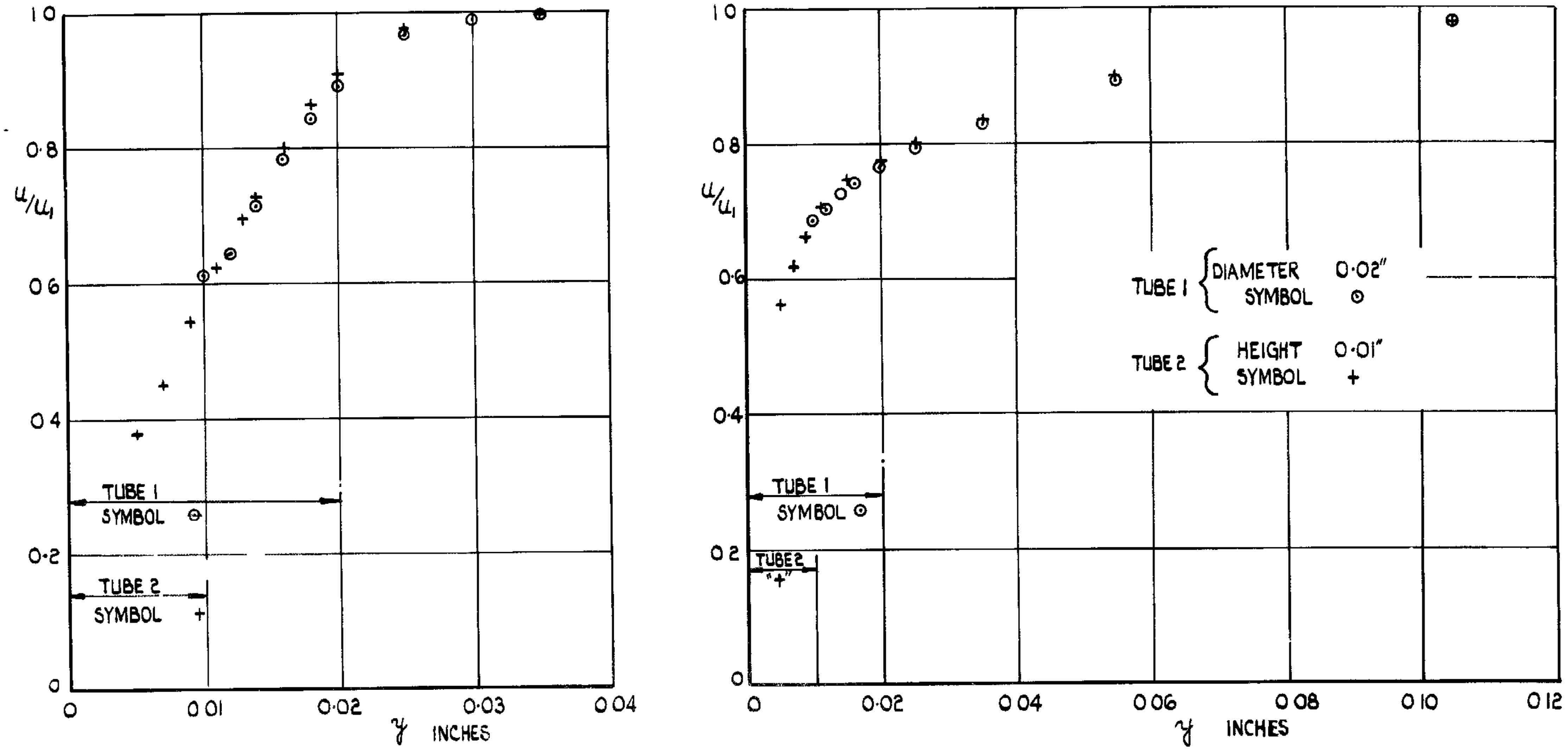

(a) LAMINAR LAYER

(b) TURBULENT LAYER.

FIG. 12. EFFECT OF PITOT TUBE SIZE ON ACCURACY OF BOUNDARY LAYER MEASUREMENTS.

FIG. 12.

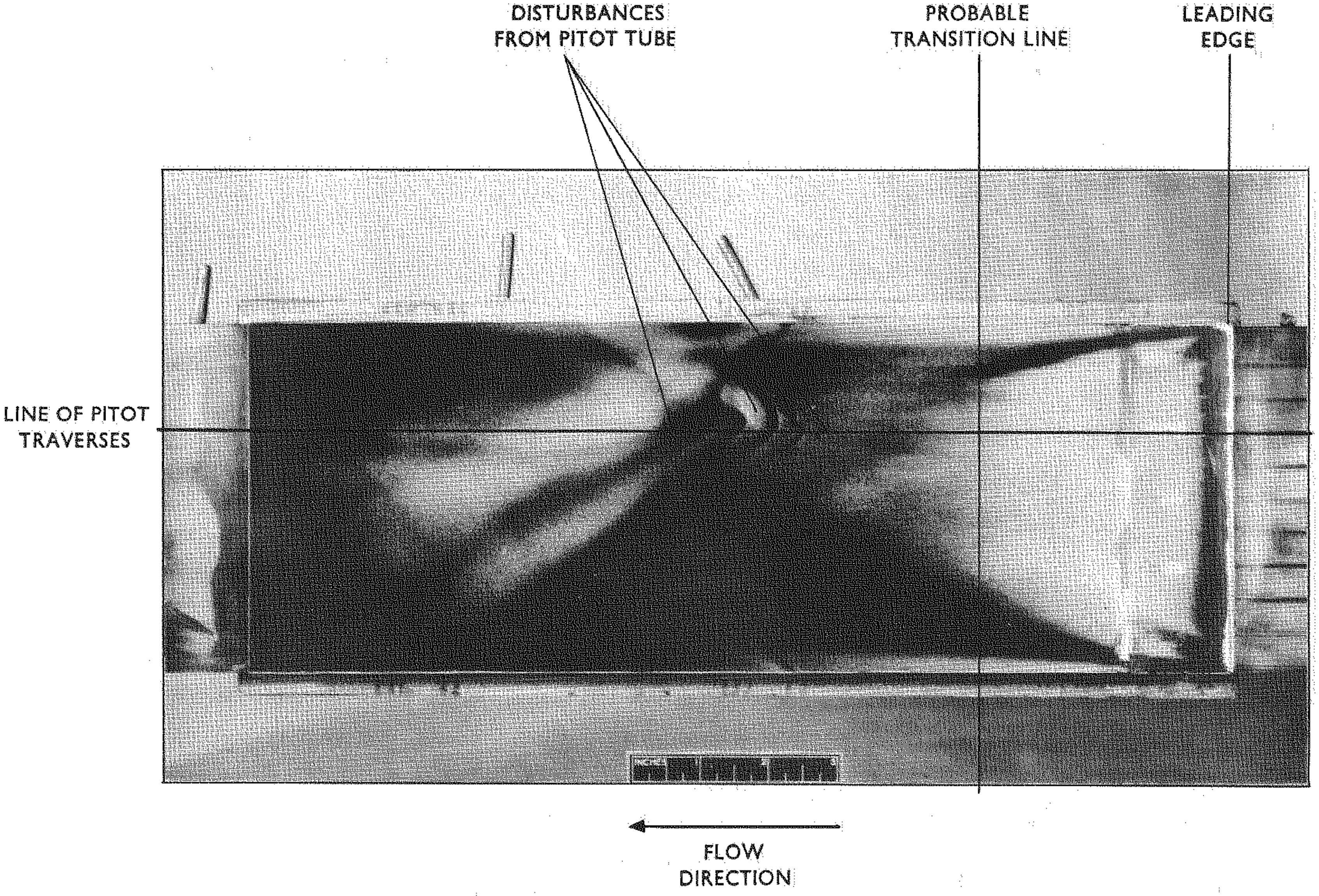
DISTURBANCES FROM PITOT TUBE
PROBABLE TRANSITION LINE
LEADING EDGE
LINE OF PITOT TRAVERSES
FLOW DIRECTION

FIG. 13. CHEMICAL INDICATION OF TRANSITION EVAPORATION METHOD USING AZOBENZENE

FIG. 13

C.P. No. 64
13064
A.R.C. Technical Report

PUBLISHED BY HIS MAJESTY'S STATIONERY OFFICE
To be purchased from
York House, Kingsway, LONDON, W.C.2, 429 Oxford Street, LONDON, W 1,
P.O. Box 569, LONDON, S.E.1,
13a Castle Street, EDINBURGH, 2. | 1 St. Andrew's Crescent, CARDIFF
39 King Street, MANCHESTER, 2 | 1 Tower Lane, BRISTOL, 1.
2 Edmund Street, BIRMINGHAM, 3. | 80 Chichester Street, BELFAST,
or from any Bookseller
1952
Price 8s. 0d. net
PRINTED IN GREAT BRITAIN

S.O. Code No. 23-9006-64